Granulation and microbial community dynamics in the chitosan-supplemented anaerobic treatment of wastewater polluted with organic solvents

K. Torres, F. J. Álvarez-Hornos, P. San-Valero, C. Gabaldón, P. Marzal*

Research Group on Environmental Engineering (GI^{2}AM), Department of Chemical Engineering, Universitat de València, Av. de la Universitat s/n, 46100, Burjassot, Spain

*Corresponding author. Paula Marzal, Department of Chemical Engineering, Universitat de València, Av. de la Universitat s/n, 46100, Burjassot, Spain. Telephone: +34963543331; fax: +34963544898

E-mail: Paula.Marzal@uv.es (P. Marzal)

URLs: http://www.uv.es/giam

Abstract

The effect of chitosan on the development of granular sludge in upflow anaerobic sludge blanket reactors (UASB) when treating wastewater polluted with the organic solvents ethanol, ethyl acetate, and 1-ethyoxy-2-propanol was evaluated. Three UASB reactors were operated for 219 days at ambient temperature with an organic loading rate (OLR) of between 0.3 kg COD m^{-3} d^{-1} and 20 kg COD m^{-3} d^{-1}. One reactor was operated without the addition of chitosan, while the other two were operated with the addition of chitosan doses of 2.4 mg $gVSS^{-1}$ two times. The three reactors were all able to treat the OLR tested with COD removal efficiencies greater than 90%. However, the time required to reach stable operation was considerably reduced in the chitosan-assisted reactors. The development of granules in the reactors with chitosan was accelerated and granules larger than 2000 μm were only observed in these reactors. In addition, these granules exhibited better physiochemical characteristics: the mean particle diameter (540 and 613 μm) was approximately two times greater than in the control reactor (300 μm), and the settling velocities exceeded 35 m h^{-1}. The extracellular polymeric substances (EPS) in the reactors with the chitosan was found to be higher than in the control reactor. The protein-EPS content has been correlated with the granule size. The analyses of the microbial communities, performed through denaturing gradient gel electrophoresis and high-throughput sequencing, revealed that the syntrophic microorganism belonging to genus *Geobacter* and the hydrogenotrophic methanogen *Methanocorpusculum labreanum* were predominant in the granules. Other methanogens like *Methanosaeta* species were found earlier in the chitosan-assisted reactors than in the control reactor.

Keywords: Chitosan, DGGE, Granulation, High-throughput sequencing, Solvents, UASB

1 Introduction

Interest in the biological treatment of industrial wastewater has increased in recent decades due to the increased pollution of water resources and its implications for human health. Among the industrial sectors, those that use organic solvents in the production of paints, adhesives, rubber, pharmaceutical and petroleum products, among others, can generate large quantities of solvent polluted wastewater (Dsikowitzky and Schwarzbauer, 2013; Oktem et al., 2007). Organic solvents are flammable, malodorous and potentially toxic to aquatic ecosystems and thus require complete elimination by wastewater treatment (Henry et al., 1996). As suitable biological wastewater treatments, the anaerobic processes have shown advantages including energy recovery as biogas and lower energy costs (van Lier, 2008). The high rate sludge bed reactors such as the Upflow Anaerobic Sludge Blanket reactor (UASB) and its derivatives are by far, the most popular anaerobic systems for the treatment of industrial wastewater because they achieve high biomass retention improving the treatment efficiency while applying high loading rates (van Lier et al., 2015; Zhou et al., 2006). Recently, this type of reactor has been successfully applied to the treatment of wastewater polluted with organic solvents (Bravo et al., 2017; Enright et al., 2009; Lafita et al., 2015; Oktem et al., 2007; Siggins et al., 2011; Wang et al., 2017).

The success of the operation of sludge bed anaerobic reactors lies in the formation and stability of granules. Granulation is the result of the self-immobilization of anaerobic microorganisms under certain physicochemical and biological conditions. Although granule formation has been widely studied, this phenomenon occurs within a limited range of wastewater characteristics and reactor designs (Uyanik et al., 2002) since the microstructure of the granules may be affected by the complexity of the substrate (Liu et al., 2002). The extracellular polymeric substances (EPS) play an important role in

granulation because they can bind cells closely through ion binding interactions, hydrophobic interactions, and polymer entanglement (Sheng et al., 2010). The EPS that result from cell secretions, cellular lysis and hydrolysis of macromolecules mainly contains polysaccharides, proteins, nucleic acids, lipids, uronic acids and humic substances, although its production and composition may be affected by the wastewater type. For example, Schmidt and Ahring (1994) indicated that the production of EPS was limited in granules grown on acetogenic and methanogenic substrates in comparison to more complex wastewaters, and Fukuzaki et al. (1995) observed greater amounts of EPS in granules grown in starch or sucrose than in ethanol or butyrate-propionate. These observations could indicate that granules are less likely to develop in the solvent polluted wastewaters. Moreover, some researchers have reported the disintegration of granules when treating mixtures containing organic oxygenated solvents (Lafita et al., 2015; Lu et al., 2015). Therefore, it has become necessary to study the granulation that occurs when treating industrial wastewater polluted with solvents in order to evaluate granule stability and the robustness of the operation. Researchers have already studied granule formation in the treatment of wastewater polluted with phenol (Ramakrishnan and Gupta, 2006), by natural rubber processing (Thanh et al., 2016), or from the kraft pulp industry (Lu et al., 2017).

The addition of cationic polymers to high rate anaerobic reactors enhances the granulation process resulting in faster granule development (Show et al., 2004). Among these cationic polymers, chitosan stands out for its availability, environmental friendliness, and biodegradability (Yang et al., 2016). Although chitosan has not been proven for its granulation effect in wastewater containing solvents, a few studies have pointed to the beneficial effect of this biopolymer when used with other substrates. El-Mamouni et al. (1998) reported that the granulation rate in UASB reactors fed with

sucrose was 2.5 times higher in the reactor containing chitosan than in the control reactor. Hudayah et al. (2016) found that in the treatment of wastewater containing glucose and volatile fatty acids (VFA) as substrates, the addition of chitosan increased the average diameter size of the granules by 115 μm.

Anaerobic granulation is a complex process in which not only physical but also biological and microbiological factors are involved (Hulshoff Pol et al., 2004). Knowledge of the microbial community implicated in the granulation of sludge that is fed with a specific substrate is essential, because it makes possible an elucidation of the potential capacities and limitations of the granules. In turn, these determine the performance and feasibility of the operation. Thus, methanogens related to the *Methanosaeta* species have been reported to be key microorganisms in anaerobic aggregation (Gagliano et al., 2017; Hulshoff Pol et al., 2004; Wiegant, 1987). In reactors in which high acetate concentrations in the effluent are maintained, *Methanosarcina* species became the dominant aceticlastic methanogens because they may resist to VFA inhibition by forming multicellular aggregates in which the VFA concentrations are limited by a slow diffusion rate (Vavilin et al., 2008). Other researchers have found that *Methanomicrobiales* play a critical role in the formation of granules at low temperature (O'Reilly et al., 2010). The presence and abundance of specific microorganisms in granular sludge depends on the type of substrate and on the operational and environmental conditions of the process, but few studies are to be found on the evolution of the microbial community during the granulation process in the treatment of wastewater containing organic solvents.

The present study aims to evaluate granulation and the dynamics of the microbial community in anaerobic reactors treating a mixture of oxygenated organic solvents when chitosan is added to assist the granulation process. To this end, three UASB

reactors fed with wastewater polluted with ethanol, ethyl acetate and 1-ethyoxy-2-propanol, as the major constituents of the emission from the flexographic industry, were operated at ambient temperature for more than 200 days. The addition of chitosan was evaluated for its effect both on the system performance and on the granulation process. The dynamics of the physicochemical characteristics of granules, such as particle size and extracellular polymer production, were examined. To gain insight into the microbiology of the process, the evolution of the microbial community was evaluated throughout the experiment by the use of molecular biology techniques.

2 Materials and methods

2.1 UASB reactors and operation

2.1.1 Experimental set-up

The experiments were carried out in three UASB reactors (R1, R2 and R3) for which a schematic diagram is shown in Fig. 1. The reactors consisted of two PVC parts: a bottom zone of 6.5 cm in diameter and 120 cm in height, and a settling zone containing the gas-liquid-solid (GLS) separator, with a diameter of 20 cm and a height of 24 cm for R1 and R2 (effective volume of 7.8 L) and 12 cm for R3 (effective volume of 4.5 L). The reactors were fed with wastewater contaminated with a mixture of ethanol, ethyl acetate and 1-ethoxy-2 propanol (E2P), with a mass ratio of 7:2:1, by using a syringe pump (New Era, 1000 model, USA). The influent was supplemented with $NaHCO_3$ so as to maintain the reactor pH between 7 and 7.5, the macronutrients in a COD:N:P ratio of 300:2:1, Ca^{+2} and Mg^{+2} to ensure 150 and 40 mg L^{-1} respectively, and micronutrients (Table Sup1). The up-flow velocity was adjusted, if necessary, by effluent recirculation

using a peristaltic pump (Watson-Marlow, USA). Biogas produced was passed through a NaOH solution to allow CO_2 absorption before being conducted to the volumetric drum-type gas flow meter MilliGascounter (Ritter TG 05, Germany).

2.1.2 Inoculum

Sludge collected from the anaerobic digester of the Quart-Benager municipal wastewater treatment plant (WWTP) located in Valencia (Spain) was used as the inoculum. The sludge had a total suspended solids (TSS) concentration of 24.6 g L^{-1} with a volatile suspended solids (VSS) content of 63%, a mean particle size of 63.7 μm and specific methanogenic activity (SMA) of 8.2 Nml CH_4 g VSS^{-1} d^{-1} for the mixture of solvents in this study.

2.1.3 Experimental procedure

The three reactors (R1, R2 and R3) were seeded with 2.5 L of inoculum and then operated at room temperature for the whole experiment (24.0 ± 1.4°C, suboptimal mesophilic temperature). R1 was operated as the control reactor without the addition of chitosan; whereas R2 and R3 were supplied with a single dose of 2.4 mg g VSS^{-1} of chitosan together with the inoculum during the seeding. Chitosan was added to the reactors using a stock solution of 10 g L^{-1} of commercial grade chitosan powder - medium molecular weight and deacetylation grade of 75% (Sigma-Aldrich, Spain)- in 1% acetic acid. The optimal chitosan dose was determined from a flocculation test (Fig. Sup1). The granulation experiment was divided into three phases and the operational parameters are summarized in Table 1. For more detail, Fig. Sup2 shows the changes of the operational parameters over time in all reactors. During phase I (days 0 to 22), considered the adaptation period for the organic solvents, the organic loading rate (OLR) was increased from 0.3 to 0.6 kg COD m^{-3} d^{-1} at a hydraulic retention time

(HRT) of 7.8 d. R1 and R2 were operated with recirculation, setting the up-flow velocity at 1 m h^{-1}. R3 was operated without recirculation. On day 23, at the beginning of phase II (days 23 to 89), a second dose of 2.4 mg g VSS^{-1} of chitosan was supplied to R2 and R3. A load of 18 g COD d^{-1} was then applied, corresponding to an OLR of 2.3 kg COD m^{-3} d^{-1} for R1 and R2, and 4 kg COD m^{-3} d^{-1} for R3. In this phase, the up-flow velocity was kept at the same value as during the previous stage. From day 90 to day 219 (phase III), the recirculation was switched off in R1 and R2 in the light of results obtained in phase II. The OLR was gradually increased in a stepwise fashion up to 20 kg COD m^3 d^{-1}. The OLR steps were performed by shortening the HRT or by increasing the load of solvents after achieving a stable performance at each OLR step (considered as variations of less than 5% in the COD removal efficiency for a period lasting at least 3 times the HRT, and VFA concentration in the effluent below 150 mg HAc L^{-1}).

2.2 Properties of the granules

2.2.1 Particle size distribution, settling velocity and morphology

Particle size distribution on a volume basis was measured every 4–5 weeks by laser diffraction using a Mastersizer 2000 (Malvern Instruments Ltd, UK) with a detection range of 0.02–2000 μm. The sludge samples were taken from each reactor and filtered through a 2 mm sieve to determine the quantity of particles with a diameter >2 mm. The fraction <2 mm was measured in the Mastersizer 2000 in triplicate. The settling velocity was determined according to the method proposed by Ghangrekar et al. (2005) using a 60 cm height PVC column with a 6 cm diameter. In addition, the morphology of the granules was analyzed using scanning electron microscopy (SEM-4100 model, Hitachi,

193 Japan). Previously, the granules samples were fixed, dried to the critical point and
194 sputter coated by Au-Pd.

195 *2.2.2 Specific Methanogenic Activity (SMA)*

196 Measurement of SMA was conducted in an automatic methane potential test system
197 (AMPTS) II (Bioprocess control, Sweden) from the biomass sampled from the reactors
198 at the end of the experiment (day 219) in order to evaluate the biodegradability of the
199 solvents in the granular sludge. The tests were carried out at 25ºC in triplicate by using
200 500 mL flasks intermittently stirred (1 min on/ 1 min off) at 112 rpm. Flasks were filled
201 with biomass and medium at a ratio of 2.5 g VSS g COD^{-1}. The medium consisted of
202 synthetic wastewater contaminated with a sole solvent (ethanol, ethyl acetate, or E2P) or
203 with the mixture, with a COD concentration of 2.5 g L^{-1}, fortified with micro and
204 macro-nutrients according to Table Sup1, and buffered at pH 7–7.5 by adding $NaHCO_3$.
205 Methane was monitored in the gas meter device, the CO_2 having been previously
206 removed by passing through a NaOH 3M solution. The SMA was evaluated as the
207 maximum specific methane production rate (Loosdrecht et al., 2016).

208 *2.2.3 Extraction and characterization of EPS*

209 The EPS of granules sampled for particle size distribution was extracted by using the
210 method proposed by Frølund et al. (1996) and modified by D'Abzac et al. (2010) using
211 a cationic exchange resin (Dowex 20–50 mesh, Sigma-Aldrich, Spain) at a ratio of 70 g
212 resin g VSS^{-1}. The polysaccharides and proteins were determined by the colorimetric
213 methods proposed by Dubois et al. (1956) and Lowry et al. (1951), respectively.

2.3 Analytical methods

Soluble COD of samples filtered by 0.22 μm, TSS and VSS were measured twice per week according to Standard Methods for the Examination of Water and Wastewater (APHA, 1998). VFA and alkalinity of centrifuged samples were daily determined according to the 5-point acid-base titration method described by Moosbrugger et al. (1992), using a titrator (848 Titrino Plus, Metrohm, Switzerland). The VFA represents the concentration of short chain volatile fatty acids, expressed as acetic acid (mg HAc L^{-1}). Effluent solvent content of samples filtered by 0.22 μm was analyzed twice per week by gas chromatography (Agilent GC 7890A, Spain) equipped with a Restek Rtx-VMS column (30 m x 0.25 mm x 1.4 μm) with helium at a flow-rate of 1.3 mL min^{-1} and a flame ionization detector (FID). The injector and detector temperatures were 190ºC and 240ºC, respectively, and oven temperature ramp was used: 60°C for 14 min and then 25°C min^{-1} to 110°C. Methane production for each reactor was monitored by the gas meter MilliGascounter (Ritter TG 05, Germany). Biogas composition was analyzed using an Agilent gas chromatograph (7820A) with thermal conductivity detector (TCD). 0.5 mL of biogas (before CO_2 absorption) was separated into two columns connected in series: HP-Plot/U (30 m x 0.32 mm x 10 μm) and HP-Molisieve (30 m x 0.32 mm x 12 μm), by using helium as a carrier at a flow-rate of 4.2 mL min^{-1}. The injector, oven and detector temperatures were 200ºC, 40ºC and 250ºC, respectively.

2.4 Microbial community analysis

Sludge samples were taken from the three reactors on days 0, 37, 89, 131, and 169. DNA was extracted from 0.5 g of sludge using a FastDNA Spin Kit for Soil Isolation (MP Biomedicals, USA) following the manufacturer's instructions and stored at -20ºC. The bacterial and archaeal 16S rRNA were amplified by PCR using the primers

proposed by Bravo et al. (2017) under the following conditions: 94ºC for 5 min, 19 cycles at 94ºC for 1 min, 65ºC for 0.5 min and 72ºC for 1 min, followed by 12 cycles for bacteria and 16 cycles for archaea of 94ºC for 1 min, 55ºC for 0.5 min, 72ºC for 1 min, and a final extension step at 72ºC for 10 min. Denaturing gradient gel electrophoresis (DGGE) analysis, subsequent band excision, purification and sequencing were done by adapting the method used by Bravo et al. (2017). In this work, a linear denaturant gradient from 25% to 60% was used and electrophoresis was performed at 60ºC and 100 V for 14 h. The V4 hyper-variable region of the extracted DNA was amplified with the universal primers 515F (5'-GTG CCA GCM GCC GCG GTA A-3') and 806R (5'-GGA CTA CHV GGG TWT CTA AT-3'). Sequencing was performed using a MiSeq System (Illumina, USA). Raw 16S rRNA gene sequences obtained were screened and trimmed by using the Quantitative Insights Into Microbial Ecology (QIIME) software with a sequence length (200 nt) and mean quality score cut-off of (25nt).

3 Results and discussion

3.1 Performance of the UASB reactors

The performance of the three reactors in terms of COD removal efficiency (RE_{COD}, defined in supplementary section) and the variation of the effluent VFA concentration are shown in Fig. 2a and 2b, respectively. After inoculation, RE_{COD} were 77, 88 and 90% in the control reactor (R1), R2 and R3, respectively (Fig. 2a). During phase I, the reactors with chitosan (R2 and R3) exhibited faster adaptation to solvents with RE_{COD} higher than 92% from day 11 onwards, whereas R1 achieved a value of 84% on day 22. The VFA concentration evolution also showed better performance in the reactors with chitosan (Fig. 2b): Values were lower than 75 mg HAc L^{-1} after nine days, and no VFA

262 was detected by the end of this phase. In R1, the VFA concentration values remained
263 between 228 and 389 mg HAc L^{-1}.

264 Phase II started on day 23 with a second dose of chitosan and an OLR increase. The
265 RE_{COD} in R1 decreased to 75% in response to the OLR increase then gradually
266 increased up to 97% towards the end of this phase according to the decrease in the VFA
267 concentration. In contrast, R2 and R3 showed stable RE_{COD} values (93 to 99%) and
268 lower VFA concentrations in the effluent than R1. The control reactor took 57 days to
269 achieve removal efficiencies higher than 92%, whereas R2 and R3 took only 11 days.
270 The results of these two phases indicated that two doses of chitosan improved the
271 acclimatization period of a flocculent sludge when treating organic solvents in UASB
272 reactors. Show et al. (2004) observed similar effect in UASB reactors fed with peptone-
273 glucose wastewater, where the addition of a single dose of a cationic polymer at a
274 concentration of 80 mg L^{-1} accelerated the start-up time. The enhancement in the start-
275 up could be explained by the earlier formation of aggregates in the chitosan-assisted
276 reactors as it will be discussed in the next section.

277 During phase III (days 90 to 219), operational conditions were changed to promote the
278 development of granules. Step increases in the OLR of up to 20 kg COD m^{-3} d^{-1} were
279 performed in each reactor according to its response. The increase in the OLR usually
280 resulted in an initial decrease in RE_{COD}; however, during stable performance at each
281 OLR step, each reactor reached a value higher than 90%, thereby demonstrating high
282 capacity to treat the solvents. Differences were observed in the performance of the three
283 reactors. For example, R1 and R2 needed 24 days to achieve a stable performance at an
284 OLR of 5 kg COD m^{-3} d^{-1}. During these 24 days, R3 was able to treat up to 10.5 kg
285 COD m^{-3} d^{-1} with an average RE_{COD} of 98%. The VFA concentration in R1 initially
286 reached 360 mg HAc L^{-1} and decreased to 69 mg HAc L^{-1} before the next OLR step was

287 applied. The VFA concentrations in R2 and R3 remained below 100 mg HAc L^{-1}. The
288 next OLR step applied in R1 and R2 (on day 119) led to a decrease of the RE_{COD} and
289 higher values of VFA in the effluent of R1 (Fig. 2b). In order to avoid the failure of this
290 reactor, the OLR was decreased until operating conditions were restored with RE_{COD}
291 higher than 85%. The response to the increase in OLR in the reactors with chitosan was
292 different to that observed in the control reactor. As can be seen in Fig. 2b, R1 showed a
293 higher oscillation in VFA concentrations with an average of 176 ± 146 mg HAc L^{-1},
294 which indicated an imbalance between acetogenesis and methanogenesis. This
295 contrasted with the chitosan-assisted reactors, where there were averages of 60 ± 63 and
296 26 ± 81 mg HAc L^{-1} for R2 and R3, respectively. The time required to reach an OLR of
297 20 kg COD m^{-3} d^{-1} was 107, 72 and 37 days for R1, R2 and R3, respectively, from the
298 beginning of the phase III. Operating at this OLR, stable RE_{COD} higher than 93% were
299 obtained for the three reactors. From day 133 to day 147, R3 operated at 25 kg COD m^{-3}
300 d^{-1}; however, excessive biomass washed out (846 mg VSS L^{-1} in the effluent) on day
301 145 and an increase of the VFA concentration was observed (Fig 2b). Therefore, the
302 OLR was gradually decreased to 20 kg COD m^{-3} d^{-1}.

303 The methane yield was determined for phase III fitting the methane produced and the
304 COD removed, obtaining values of 0.292±0.008, 0.323±0.004 and 0.335±0.005 Nm^3
305 CH_4 kg $COD_{removed}^{-1}$ for R1, R2, and R3, respectively. The values from the reactors with
306 chitosan were closer to the stoichiometric value (0.35 Nm^3 CH_4 kg $COD_{removed}^{-1}$).

307 The analysis of the solvent content in the effluent throughout the study showed that the
308 only remarkable compound detected was 1-ethoxy-2-propanol (E2P). Ethanol and ethyl
309 acetate were almost completely degraded, with their concentrations always below 10
310 ppm. Intermediate compounds such as acetone and isopropanol were also detected (<10
311 ppm). Bravo et al. (2017) hypothesized that E2P would be decomposed after enzymatic

ether cleavage to ethanol and acetone. This assumption is corroborated by the low concentrations of acetone measured in the effluents of the reactors. The variations in the E2P removal efficiency (RE_{E2P}, defined in supplementary section) according to the OLR of this solvent are shown in Fig. 3. The reactors with chitosan were able to achieve RE_{E2P} of 79% from day 14 onwards; while the control reactor needed 40 days to achieve values of around 70%. During phase III, the control reactor showed more oscillations in behavior related to E2P degradation, and at the final E2P OLR of 2 kg COD m^{-3} d^{-1}, average removal percentages of 62±8, 70±3 and 71±2 were obtained in R1, R2, and R3, respectively. The outcomes of the reactors' performance suggest that the addition of chitosan enhances the adaptation of UASB reactors to the degradation of solvents, including a complex one such as E2P, improving the overall performance and the robustness of the system.

3.2 Development of granules

The development of granules throughout the study was evaluated from biomass samples from the three reactors taken on days 0, 22, 54, 89, 112, 131, 169, 190 and 219. The evolution of the particle size distribution is presented in Fig. 4. In this study, particles with a diameter greater than 300 μm were considered to be granules, in the order of the minimum granules diameter indicated by Bhunia and Ghangrekar (2007). Table 2 summarizes the percentage of granules over time in all reactors. After 22 days of operation, the percentage of granules increased significantly from 0.3% to values of 3.0, 4.0 and 6.8% in R1, R2 and R3, respectively. After the second addition of chitosan on day 23, the samples taken during phase II showed that R3, operating with chitosan and without recirculation, presented a greater granulation rate; between the reactors operated

with recirculation, the chitosan-assisted reactor (R2) reached a percentage of granules greater than that obtained in the reactor without chitosan (R1). At the end of this phase, on day 89, the percentage of granules in R3 was 21.9%, while a low increase in granules was observed for R1 and R2 with 4.9 and 8.5%, respectively. In addition, the samples taken on this day show that the percentage of fine particles (<100 μm) in R3 decreased by half, whereas that in R1 and R2 it only decreased 11 and 15%, respectively. According to the granulation theory, the selection pressure created by the hydraulic and gas loading rates induces the washing out of light and dispersed sludge particles, while the heavier components remain in the system promoting sludge granulation (Hulshoff Pol et al., 2004). However, during phase II, the sludge blanket in R1 and R2 was often observed to be accumulated in the settling zone, with subsequent recirculation and low washing out of fine particles with the effluent. Hence, the almost unvaried particle size distribution could be the result of retaining the fine particles instead of promoting their washing out. It was therefore decided that the recirculation in R1 and R2 would be switched off, so that during phase III all three reactors were operated without recirculation and with stepwise increases in the OLR. Under these conditions the granules grew faster in the chitosan-assisted reactors, and larger granules were observed in comparison to the control reactor. On day 112 (22 days after the starting of the phase III) the percentage of granules in R1 did not show significant variation (4.9%), while in R2 and R3 it was 22.7% and 24.5%, respectively, showing the enhancement of the granulation in the chitosan-assisted reactors. From that point onwards, the percentage of granules increased until values of 42.0% in R1, 54.0% in R2, and 64.7% in R3. Regarding the granule size (Figure 4), granules larger than 1000 μm appeared earlier in the chitosan assisted-reactors, and granules > 2000 μm were only found in these reactors. At the end of the study, the mean particle diameter was significantly higher in

361 R2 and R3, with values of 540 μm and 613 μm respectively, compared with 300 μm
362 obtained in R1. The results showed that granulation was possible in all three reactors
363 when a high selection pressure was applied, which was induced by a gradual increase in
364 the organic loading rate. However, the granules formation was improved in the
365 chitosan-assisted reactors, with a consequent increase of biomass retention and of the
366 methanogenic activity in turn. Yang et al. (2016) have suggested that the main
367 mechanisms of microbial flocculation in the presence of chitosan are related to charge
368 neutralization and bridging.

369 A significant parameter in the quality of the granular sludge is its settling velocity.
370 Granules from the control reactor measured on day 219 presented a settling velocity of
371 26.4 m h^{-1}, but the granules from the reactors with chitosan, R2 and R3, exhibited better
372 settling velocities with 1.4 (36.7 m h^{-1}) and 1.8 (46.8 m h^{-1}) times higher values,
373 respectively. The fact that granules were formed earlier and with better physical
374 characteristics in the chitosan-assisted reactors could be attributed to a higher retention
375 of microorganisms inside the matrix formed by the polymer. To evaluate this
376 assumption, scanning electron microscopy (SEM) images were obtained from the
377 granules on day 219. Fig. 5a and 5b show the granules formed in R1 and in R3 (R2 had
378 a similar appearance), respectively. The granules developed in all three reactors were
379 rigid and densely packed with a smooth surface. The granules from R3 showed the
380 typical EPS formations embedding diverse arrangements of microorganism (Fig. 5d),
381 whereas in R1 such EPS formations were not directly observed in the SEM images. The
382 magnification of the granules' surface showed a heterogeneous microbial community:
383 cocci, rods and filamentous microorganisms were observed, these last ones identified to
384 a greater extent in the reactors with chitosan added. *Methanosaeta* rods- (Fig 5.c) and

385 rods/filaments-like morphology (Fig 5.d) can be seen, being more abundant in the
386 chitosan-assisted reactor.

387

388 3.3 EPS Production

389 Table 3 shows the evolution of the EPS content, which involved both polysaccharides
390 and proteins, in the three UASB reactors. After the acclimation period, an increase in
391 the OLR in phase II resulted in a sharp increase to the polysaccharide-EPS content,
392 although it decreased by the end of this phase. This behavior corresponded to the
393 increase in the VFA concentration caused by the increase in the OLR, which is in
394 agreement with several studies indicating that OLR-stressful conditions promote EPS
395 production (Puñal et al., 2003; Zhou et al., 2006). Once the system became stable,
396 polysaccharide-EPS production decreased again. From day 112 on, with successive
397 increments in the OLR, the polysaccharide-EPS content of the three reactors increased,
398 although it did so to a higher extent in the reactors with added chitosan. This may be
399 related to the more rapid increases in the OLR that occurred in these reactors.

400 The protein-EPS content of R2 and R3 showed higher values than that of the control
401 reactor; the values increased in relation to the formation of granules. From day 131
402 onwards, a sharp increase in protein-EPS content was observed as larger granules
403 appeared, suggesting a correlation between the protein-EPS content and the granulation
404 process (Fig. Sup3). Zhang et al. (2007) also observed an increase of the protein-EPS
405 content as aerobic granulation occurred. These authors suggested that the increase of the
406 protein might favor the granulation by affecting the relative hydrophobicity of cell
407 surfaces and by reducing the electrostatic repulsion between cells.

408

3.4 Specific Methanogenic Activity (SMA)

At the end of the experiment, SMA assays for the granular sludge taken from the three reactors were carried out using a sole solvent or the ternary mixture as substrate. These results are presented in Table 4. Higher methanogenic activities were evident in the sludge from the chitosan-assisted for all substrates evaluated. Similar results were observed by El-Mamouni (1998). The SMA values obtained in this study were higher than others reported at suboptimal mesophilic temperature when using a granular sludge adapted to organic solvents. For instance, Lafita et al. (2015) reported an SMA of 214.5 NmL CH_4 g VSS^{-1} d^{-1} for ethanol and of 24.3 NmL CH_4 g VSS^{-1} d^{-1} for 1-methoxy-2-propanol at 25°C. Ethyl acetate has been described as a readily biodegradable solvent under anaerobic conditions (Henry et al., 1996). Yanti et al. (2014) suggest that the mechanism of ethyl ester degradation is the same as that of methyl ester, i.e., these compounds are degraded to carboxylic acids and alcohols. Following this process, ethyl acetate would be transformed into acetic acid and ethanol, and it seems that this step could be the kinetically limiting one because of the slightly lower values of SMA for ethyl acetate than for ethanol. The SMA values obtained for E2P were significantly lower (an average of 5 times) than the values observed for the other two solvents (ethanol and ethyl acetate). In addition, no lag phase was observed in its degradation, suggesting the presence of a well-established population of microorganisms capable of producing the ether cleaving enzymes for the uptake of this glycol ether. Regarding the SMA assay for the mixture, different slopes in the methane production during the degradation of the three compounds were not observed; i.e., a constant SMA was observed during the whole test, and similar values of SMA as those observed for the more biodegradable solvents were achieved.

3.5 Microbial community analysis

Fig. 6 shows the DGGE banding patterns for the bacterial (Fig. 6a) and archaeal (Fig. 6b) populations of the sample taken from the inoculum and the samples taken from the three UASB reactors at days 37, 89, 131 and 169 of the operation. The bands indicated in Fig. 6 were excised and sequenced. Table 5 summarizes their designation, the level of similarity to related GenBank sequences and the phylogenetic affiliations of each strain.

A total of seventeen predominant bands were excised from the bacterial DGGE (Fig. 6a): four corresponding to the seed sludge and thirteen to the UASB reactors. The DGGE pattern showed a shift in the bacterial populations of the reactors relative to the inoculum, and only one of the bands observed initially (B7) remained in the three reactors throughout the experiment. This shift was related to the different operational and environmental conditions of our experiment compared to those applied in the anaerobic digester source of the seed sludge.

Bands B7 and B16 were identified as *Geobacter psychrophilus* and *Geobacter chapellei*, respectively. These microorganisms, which were present in all three reactors, can oxidize substrates such as ethanol, acetate, formate or lactate, coupled with the reduction of iron or manganese oxides (Coates et al., 2001; Nevin et al., 2005). *Geobacter* species are known to be specialists in making electrical connections with extracellular electron acceptors and other organisms, such as *Methanosaeta*, based on the direct interspecies electron transfer (DIET) mechanism (Shen et al., 2016). Band B10 was affiliated with *Pelobacter propionicus*. This microorganism has been reported to produce acetate and propionate from ethanol (Schink et al., 1987) and has been found to be involved in the syntrophic oxidation of primary alcohols and diols with hydrogen-utilizing partners via the interspecies H_2 transfer mechanism (Shen et al., 2016). Band

B11 was associated with *Smithella propionica*, which is a species of syntrophic propionate-oxidizing bacteria that produces small amounts of butyrate with H_2 or formate-using methanogenic partners in addition to acetate (Liu et al., 1999). These bacteria, which are involved in the syntrophic production and consumption of VFA, were not observed in the seed sludge, but their intensity (especially B10) became stronger in the three reactors once the granulation process had progressed, being observed earlier in the reactors with chitosan.

Band B12 was related to *Treponema caldarium.* These bacteria are possibly homoacetogens, which are able to consume H_2 and CO_2 to produce acetate (Zhang et al., 2009). The intensity of this band was very low compared to those of the *Pelobacter* and *Smithella*, which suggests that the H_2 produced in our reactors was mainly utilized in syntrophic associations with hydrogenotrophic methanogens.

The phylum *Firmicutes* was represented by bands B8 and B15. The first band was related to *Clostridium* sp., which are commonly present in methanogenic environments (Díaz et al., 2006). Band B15 was affiliated with *Trichococcus pasteurii*, an aerotolerant fermentative organism growing with glucose, sucrose and lactose to produce lactate, acetate, formate and other acids, which has previously been found in anaerobic bioreactors operated at low temperature (Bialek et al., 2014). Although the intensity of band B15 was low throughout the experiment, it could have been favored due to the operational temperature established (24.0 ± 1.4°C). The bands corresponding to the phylum *Bacteroidetes* were related to the genus *Capnocytophaga* (B9, B13 and B17) and *Flavobacterium* (B14). These microorganisms are facultative anaerobes. They have been previously found in anaerobic reactors treating acidogenic substrates or municipal sludge (Li et al., 2016; Maspolim et al., 2015; Zhao et al., 2016).

Regarding the archaeal community, a total of nine bands were excised and identified (Fig. 6b and Table 5). Some differences were observed between the control reactor and those inoculated with chitosan, which could explain how the polymer accelerated the granulation process. Although almost all the bands identified in the inoculum remained in all samples throughout the experiment, it is remarkable that bands A3 and A5 were not observed on day 37 in R1, while in the reactors inoculated with chitosan, these bands were present. Bands A3 and A5 are closely related to the *Methanosaeta* species. *Methanosaeta* is a well-known acetotrophic methanogen described as a key microorganism in the granulation processes in which it acts as a nucleation center (Macleod et al., 1990). It seems that chitosan can help retain these microorganisms, as Khemkao et al. (2011) observed while treating palm oil mill wastewater in an UASB reactor to which chitosan had been added at the start-up. Therefore, the higher population of acetotrophic methanogens could explain the improved performance of the reactors that were inoculated with chitosan. As previously indicated, several studies have found that DIET can occur between *Geobacter* and *Methanosaeta* species within aggregates from anaerobic reactors treating wastewaters with a high content of ethanol, such as brewery wastewaters (Morita et al., 2011; Rotaru et al., 2014; Shrestha et al., 2014). Therefore, it could be assumed that DIET interactions were present in the aggregates from our reactors, since ethanol was the main solvent in the synthetic wastewater we applied as well as an intermediate in the degradation of ethyl acetate and 1-ethoxy-2-propanol, which were the other solvents in the reactors feeding stream.

The predominant band found in the archaeal DGGE in all biomass samples during the experiment was band A1, which was identified as *Methanocorpusculum labreanum*, a hydrogenotrophic archaea related to the granulation process in high-rate anaerobic reactors operating at a low temperature (O'Reilly et al., 2009). The operation of our

reactors at sub-mesophilic temperatures favored the prevalence of this organism, which increased in abundance from day 37 until the end of the experiment. Band A2 was identified as *Methanospirillum hungatei*, which is a hydrogenotrophic methanogen associated with *Pelobacter* bacteria in the syntrophic degradation of primary alcohols and diols (Eichler and Schink, 1985). This band was present in the inoculum but was not observed in any reactor at any other time, despite the fact that ethanol was the main solvent in the feeding synthetic wastewater and *Pelobacter* was observed throughout the experiment in all the reactors. The operational conditions and the predominance of other hydrogen-utilizing microorganisms belonging to the *Methanomicrobiales* order, such as *Methanoscorpulum*, could limit the growth of the *Methanospirillum* species.

The order *Methanobacteriales* was represented by *Methanobacterium beijingense* (A6). This hydrogenotrophic archaea was detected in all reactors from day 89 onwards. Its abundance remained stable, according to the intensity of the bands, until the end of the trial. *Methanobacterium beijingense* was isolated from an anaerobic digester for the treatment of beer-manufacture wastewater (Ma et al., 2005) and has been found in anaerobic reactors treating organic solvents in phenol or trichloroethylene-contaminated wastewater at a broad range of temperatures (15 to 37°C; Chen et al., 2008; Siggins et al., 2011). Band A7 was closely related to *Methanosarcina mazei.* This acetoclastic methanogen could compete with *Methanosaeta* depending on the acetate concentration, being predominant at high concentrations (Conklin et al., 2006; McMahon et al., 2001; Wiegant, 1987). *Methanosarcina mazei* was only identified on day 89 in the control reactor, but it was not observed afterwards. Although the control reactor had eventual peaks of VFA during phase III, the average VFA concentration remained below 200 mg HAc L^{-1}, thus favoring the dominance of *Methanosaeta* over *Methanosarcina.*

530 The biomass sample taken from the inoculum and the granular samples taken from the
531 three UASB reactors at day 169 were analyzed by high-throughput sequencing. A
532 summary of the microbial community structure at phylum level is plotted in Fig. Sup4.
533 The dominant phyla detected in relative abundances higher than 1% of total sequences
534 in at least one sample include *Euryarchaeota*, *Actinobacteria*, *Bacteroidetes*,
535 *Chloroflexi*, *Firmicutes*, *Proteobacteria*, *Synergistetes* and *Cloacimonetes*. Results show
536 a shift in the microbial communities from the inoculum to the granular sludge of the
537 three UASB reactors throughout the operation. The microbial communities observed in
538 all reactors at day 169 are quite similar as same wastewater composition was used. The
539 *Euryarchaeota* phylum that includes the methanogenic microorganisms became highly
540 dominant in the granular samples. This phylum increases its relative abundance from a
541 value of 0.31% in the inoculum to values in the chitosan-assisted reactors, R2 and R3,
542 of 32.39% and 33.60%, respectively, with greater abundances than that obtained in the
543 control reactor, 29.90%. Other dominant phyla as *Firmicutes* decreased the relative
544 abundance during the course of the experiment in all reactors, whereas *Proteobacteria*
545 increased the abundance. *Actinobacteria* and *Chlorofelxi* phylum, with percentage
546 greater than 5% in the inoculum, almost disappeared in the three reactors throughout the
547 operation. The relative abundance of the dominant genera (with a relative abundance
548 higher than 0.1% at least in one sample) is presented in Fig. 7. Several genera related to
549 bacteria as *Coprothermobacter*, *Clostridium*, *Anaerobaculum* and *W5* with relative
550 abundances of 5.1%, 1.3%, 3.0% and 6.3%, respectively, in the initial biomass almost
551 disappeared at day 169; whereas other bacteria genera grew in the same period reaching
552 significant abundance in the three reactors. For example, *Geobacter* genus had an
553 abundance ranging between 4.1 and 7.3% in the granular samples while in the inoculum
554 the abundance was 0.2%. The genus *Syntrophus* also increased the abundance until

555 values within 1–3.4% from a value lower than 0.1% in the inoculum. This genus,
556 detected by high-throughput sequencing, belongs to *Syntrophaceae* family as same as
557 genus *Smithella* (detected by DGGE). *Pelobacter* genus was also detected in the three
558 reactors. These genera are associated to syntrophic communities of bacteria and
559 methanogenic archaea. The importance of syntrophic communities in high-rate
560 methanogenic reactors has been pointed out by Stams et al. (2012), who have indicated
561 that aggregation reduces the distance between the bacteria and methanogens favoring
562 the transfer of metabolites, which is essential to achieve high conversion rates. The
563 archaeal communities of the inoculum and the three reactors on day 169 matched those
564 obtained from DGGE. They were composed mainly with four genera:
565 *Methanobacterium*, *Methanobrevibacter*, *Methanocorpusculum* and *Methanosaeta*, with
566 an increase in their relative abundance in the granules in comparison with the inoculum.
567 The *Methanocorpusculum* was the most abundant genus in the granular sludge with
568 values of 25.3%, 30.1% and 31.7% in R1, R2 and R3, respectively. The other archaea
569 genera reached values within 0.5-1.5% in all reactors.

570 Recently, Bravo et al. (2017) reported that *Methanosaeta*, together with
571 *Methanospirillum* and *Methanobacterium*, were the predominant species in granules
572 from a pilot EGSB reactor treating industrial solvent wastewater with a similar
573 composition to that of the synthetic wastewater employed in this study. In our reactors,
574 the *Methanocorpusculum*, *Methanobacterium* and *Methanosaeta* species were found to
575 be the predominant archaea. Since the first microorganism was present in the inoculum
576 and its abundance remained throughout the study, it can be inferred that the origin of the
577 biomass source, as well as the environmental and operational conditions applied during
578 the experiment, could influence significantly the microbial community established for
579 the degradation of similar substrates.

4 Conclusion

In this study, three UASB reactors treating wastewater polluted with ethanol, ethyl acetate and 1-ethoxy-2-propanol were successfully operated. The following main conclusions can be obtained.

- Chitosan addition improved the start-up and the overall performance of the UASB reactors inoculated with flocculent anaerobic sludge and operated up to an OLR of 20 kg COD m^{-3} d^{-1}. The chitosan-assisted reactors achieved removal efficiencies >92% in only 11 days and showed more stable behavior.
- The solvent 1-ethoxy-2-propanol was successfully degraded, although with significantly lower SMA value in comparison with ethanol and ethyl acetate.
- Granulation was successfully achieved in a shorter time in the UASB reactors supplied with chitosan with larger granules appearing earlier. The granules of the chitosan-assisted reactors exhibited better settling velocities (>35 m h^{-1}), higher methanogenic activities and higher content of EPS.
- DGEE and high-throughput sequencing results showed the shift of microbial community to increase the relative abundance of Archaea. After 169 days, the three reactors presented similar microbial community due to the treatment of the same solvents. *Geobacter* and *Methanocorpusculum* were the dominant genera of the microbial community degrading anaerobically ethanol, ethyl acetate and 1-ethoxy-2-propanol.

5 Acknowledgments

Financial support was obtained from the Ministerio de Economía y Competitividad (Spain, project CTM2014-54517-R, co-financed with FEDER funds) and from the Generalitat Valenciana (Spain, project: PROMETEO/2013/053). The authors are grateful to Pablo Ferrero for his support in the microbiological analysis. Keisy Torres acknowledges to the Generalitat Valenciana for the Santiago Grisolía Grant (Grisolía/2015/A/021). We would like to thank the Unidad de Genómica del Servei Central de Suport a la Investigació Experimental at the Universitat de València for performing the high-throughput sequencing.

611

612 **References**

613 APHA, 1998. Standard methods for the examination of water and wastewater, 20th ed.
614 American Public Health Association, Washington, DC.

615 Bhunia, P., Ghangrekar, M.M., 2007. Required minimum granule size in UASB reactor
616 and characteristics variation with size. Bioresour. Technol. 98, 994–999.
617 doi:10.1016/j.biortech.2006.04.019

618 Bialek, K., Cysneiros, D., O'Flaherty, V., 2014. Hydrolysis, acidification and
619 methanogenesis during low-temperature anaerobic digestion of dilute dairy
620 wastewater in an inverted fluidised bioreactor. Appl. Microbiol. Biotechnol. 98,
621 8737–8750. doi:10.1007/s00253-014-5864-7

622 Bravo, D., Ferrero, P., Penya-roja, J.M., Àlvarez-Hornos, F. Javier Gabaldon, C.,
623 Álvarez-Hornos, F.J., Gabaldón, C., 2017. Control of VOCs from printing press air
624 emissions by anaerobic bioscrubber: performance and microbial community of an
625 on-site pilot unit. J. Environ. Manage. 197, 287–295.
626 doi:10.1016/j.jenvman.2017.03.093

627 Chen, C.L., Wu, J.H., Liu, W.T., 2008. Identification of important microbial
628 populations in the mesophilic and thermophilic phenol-degrading methanogenic
629 consortia. Water Res. 42, 1963–1976. doi:10.1016/j.watres.2007.11.037

630 Coates, J.D., Bhupathiraju, V.K., Achenbach, L.A., Mcinerney, M.J., Lovley, D.R.,
631 2001. Geobacter hydrogenophilus, Geobacter chapellei and Geobacter grbiciae,
632 three new, strictly anaerobic, dissimilatory Fe(III)-reducers. Int. J. Syst. Evol.
633 Microbiol. 51, 581–588.

634 Conklin, A., Stensel, H.D., Ferguson, J., 2006. Growth Kinetics and Competition
635 Between Methanosarcina and Methanosaeta in Mesophilic Anaerobic Digestion.
636 Water Environ. Res. 78, 486–496. doi:10.2175/106143006X95393

637 D'Abzac, P., Bordas, F., Van Hullebusch, E., Lens, P.N.L., Guibaud, G., 2010.
638 Extraction of extracellular polymeric substances (EPS) from anaerobic granular
639 sludges: Comparison of chemical and physical extraction protocols. Appl.
640 Microbiol. Biotechnol. 85, 1589–1599. doi:10.1007/s00253-009-2288-x

641 Díaz, E.E., Stams, A.J.M., Amils, R., Sanz, J.L., 2006. Phenotypic properties and
642 microbial diversity of methanogenic granules from a full-scale upflow anaerobic
643 sludge bed reactor treating brewery wastewater. Appl. Environ. Microbiol. 72,
644 4942–4949. doi:10.1128/AEM.02985-05

645 Dsikowitzky, L., Schwarzbauer, J., 2013. Organic Contaminants from Industrial
646 Wastewaters: Identification, Toxicity and Fate in the Environment, in: Lichtfouse,
647 E., Schwarzbauer, J., Robert, D. (Eds.), Pollutant Diseases, Remediation and
648 Recycling. Springer International Publishing, Cham, pp. 45–101. doi:10.1007/978-
649 3-319-02387-8_2

650 Dubois, M., Gilles, K. a., Hamilton, J.K., Rebers, P. a., Smith, F., 1956. Colorimetric
651 method for determination of sugars and related substances. Anal. Chem. 28, 350–

652 356. doi:10.1021/ac60111a017

653 Eichler, B., Schink, B., 1985. Fermentation of primary alcohols and diols and pure
654 culture of syntrophically alcohol-oxidizing anaerobes. Arch. Microbiol. 143, 60–
655 66. doi:10.1007/BF00414769

656 El-Mamouni, R., Leduc, R., Guiot, S.R., 1998. Influence of synthetic and natural
657 polymers on the anaerobic granulation process. Water Sci. Technol. 38, 341–347.
658 doi:10.1016/S0273-1223(98)00710-0

659 Enright, A.M., McGrath, V., Gill, D., Collins, G., O'Flaherty, V., 2009. Effect of seed
660 sludge and operation conditions on performance and archaeal community structure
661 of low-temperature anaerobic solvent-degrading bioreactors. Syst. Appl.
662 Microbiol. 32, 65–79. doi:10.1016/j.syapm.2008.10.003

663 Frølund, B., Palmgren, R., Keiding, K., Nielsen, P.H., 1996. Extraction of extracellular
664 polymers from activated sludge using a cation exchange resin. Water Res. 30,
665 1749–1758. doi:10.1016/0043-1354(95)00323-1

666 Fukuzaki, S., Nishio, N., Nagai, S., 1995. High rate performance and characterization of
667 granular methanogenic sludges in upflow anaerobic sludge blanket reactors fed
668 with various defined substrates. J. Ferment. Bioeng. 79, 354–359.
669 doi:10.1016/0922-338X(95)93994-U

670 Gagliano, M.C.C., Ismail, S.B.B., Stams, A.J.M.J.M., Plugge, C.M.M., Temmink, H.,
671 Van Lier, J.B.B., 2017. Biofilm formation and granule properties in anaerobic
672 digestion at high salinity. Water Res. 121, 61–71.
673 doi:10.1016/j.watres.2017.05.016

674 Ghangrekar, M.M., Asolekar, S.R., Joshi, S.G., 2005. Characteristics of sludge
675 developed under different loading conditions during UASB reactor start-up and
676 granulation. Water Res. 39, 1123–1133. doi:10.1016/j.watres.2004.12.018

677 Henry, M.P., Donlon, B.A., Lens, P.N., Colleran, E.M., 1996. Use of anaerobic hybrid
678 reactors for treatment of synthetic pharmaceutical wastewaters containing organic
679 solvents. J. Chem. Technol. Biotechnol. 66, 251–264. doi:10.1002/(SICI)1097-
680 4660(199607)66:3<251::AID-JCTB496>3.0.CO;2-S

681 Hudayah, N., Suraraksa, B., Chaiprasert, P., 2016. Synergistic effects of the chitosan
682 addition and polysaccharides-EPS on the formation of anaerobic granules. Environ.
683 Technol. 3330, 1–10. doi:10.1080/09593330.2016.1160957

684 Hulshoff Pol, L.W., De Castro Lopes, S.I., Lettinga, G., Lens, P.N.L., 2004. Anaerobic
685 sludge granulation. Water Res. 38, 1376–1389. doi:10.1016/j.watres.2003.12.002

686 Khemkhao, M., Nuntakumjorn, B., Techkarnjanaruk, S., Phalakornkule, C., 2011.
687 Effect of chitosan on UASB treating POME during a transition from mesophilic to
688 thermophilic conditions. Bioresour. Technol. 102, 4674–4681.
689 doi:10.1016/j.biortech.2011.01.032

690 Lafita, C., Penya-roja, J.M., Gabaldón, C., 2015. Anaerobic removal of 1-methoxy-2-
691 propanol under ambient temperature in an EGSB reactor. Bioprocess Biosyst. Eng.
692 38, 2137–2146. doi:10.1007/s00449-015-1453-0

693 Li, Y., Zhang, Y., Zhao, Z., Sun, S., Quan, X., Zhao, H., 2016. Enhancement of sludge
694 granulation in hydrolytic acidogenesis by denitrification. Appl. Microbiol.
695 Biotechnol. 100, 3313–3320. doi:10.1007/s00253-015-7194-9

696 Liu, Y., Balkwill, D.L., Henry, C.A., Drake, G.R., Boone, D.R., 1999. Characterization
697 of the anaerobic propionate- degrading syntrophs Smithella propionica. Int. J. Syst.
698 Bacteriol. 49, 545–556. doi:10.1099/00207713-49-2-545

699 Liu, Y., Xu, H. Lou, Show, K.Y., Tay, J.H., 2002. Anaerobic granulation technology for
700 wastewater treatment. World J. Microbiol. Biotechnol. 18, 99–113.
701 doi:10.1023/A:1014459006210

702 Loosdrecht, M.C.M. van, Nielsen, P.H., Lopez-Vazquez, C.M., Brdjanovic, D., 2016.
703 Experimental Methods in Wastewater Treatment, IWA Publishing.

704 Lowry, O.H., Rosebrough, N.J., Farrr, A.L., Randall, R.J., 1951. Protein measurement
705 with the Folin phenol reagent. J. Biol. Chem. 193, 265–75.

706 Lu, X., Zhen, G., Chen, M., Kubota, K., Li, Y.Y., 2015. Biocatalysis conversion of
707 methanol to methane in an upflow anaerobic sludge blanket (UASB) reactor:
708 Long-term performance and inherent deficiencies. Bioresour. Technol. 198, 691–
709 700. doi:10.1016/j.biortech.2015.09.073

710 Lu, X., Zhen, G., Ni, J., Kubota, K., Li, Y.Y., 2017. Sulfidogenesis process to
711 strengthen re-granulation for biodegradation of methanolic wastewater and
712 microorganisms evolution in an UASB reactor. Water Res. 108, 137–150.
713 doi:10.1016/j.watres.2016.10.073

714 Ma, K., Liu, X., Dong, X., 2005. Methanobacterium beijingense sp. nov., a novel
715 methanogen isolated from anaerobic digesters. Int. J. Syst. Evol. Microbiol. 55,
716 325–329. doi:10.1099/ijs.0.63254-0

717 Macleod, F.A., Guiot, S.R., Costerton, J.W., Hp, C., 1990. Layered Structure of
718 Bacterial Aggregates Produced in Anaerobic Sludge Bed and Filter Reactor
719 Upflow. Appl. Environ. Microbiol. 56, 1598–1607.

720 Maspolim, Y., Zhou, Y., Guo, C., Xiao, K., Ng, W.J., 2015. Comparison of single-stage
721 and two-phase anaerobic sludge digestion systems - Performance and microbial
722 community dynamics. Chemosphere 140, 54–62.
723 doi:10.1016/j.chemosphere.2014.07.028

724 McMahon, K.D., Stroot, P.G., Mackie, R.I., Raskin, L., 2001. Anaerobic codigestion of
725 municipal solid waste and biosolids under various mixing conditions - II:
726 Microbial population dynamics. Water Res. 35, 1804–1816. doi:10.1016/S0043-
727 1354(00)00439-5

728 Moosbrugger, R., Wentzel, M., Ekama, G., 1992. Simple titration procedures to
729 determine H2CO3 alkalinity and short-chain fatty acids in aqueous solutions
730 containing known concentration sulphide weak acid/bases. South African Res.
731 Com. Rep.

732 Morita, M., Malvankar, N.S., Franks, A.E., Summers, Z.M., Giloteaux, L., Rotaru, A.E.,
733 Rotaru, C., Lovley, D.R., 2011. Potential for Direct Interspecies Electron Transfer
734 in Methanogenic Wastewater Digester Aggregates. MBio 2, e00159-11.

735 doi:10.1128/mBio.00159-11.Editor

736 Nevin, K.P., Holmes, D.E., Woodard, T.L., Hinlein, E.S., Ostendorf, D.W., Lovley,
737 D.R., 2005. Geobacter bemidjiensis sp. nov. and Geobacter psychrophilus sp. nov.,
738 two novel Fe(III)-reducing subsurface isolates. Int. J. Syst. Evol. Microbiol. 55,
739 1667–1674. doi:10.1099/ijs.0.63417-0

740 O'Reilly, J., Lee, C., Chinalia, F., Collins, G., Mahony, T., O'Flaherty, V., 2010.
741 Microbial community dynamics associated with biomass granulation in low-
742 temperature (15 ^{o}C) anaerobic wastewater treatment bioreactors. Bioresour.
743 Technol. 101, 6336–6344. doi:10.1016/j.biortech.2010.03.049

744 O'Reilly, J., Lee, C., Collins, G., Chinalia, F., Mahony, T., O'Flaherty, V., 2009.
745 Quantitative and qualitative analysis of methanogenic communities in
746 mesophilically and psychrophilically cultivated anaerobic granular biofilims.
747 Water Res. 43, 3365–3374. doi:10.1016/j.watres.2009.03.039

748 Oktem, Y.A., Ince, O., Sallis, P., Donnelly, T., Ince, B.K., 2007. Anaerobic treatment of
749 a chemical synthesis-based pharmaceutical wastewater in a hybrid upflow
750 anaerobic sludge blanket reactor. Bioresour. Technol. 99, 1089–1096.
751 doi:10.1016/j.biortech.2007.02.036

752 Puñal, A., Brauchi, S., Reyes, J.G., Chamy, R., 2003. Dynamics of extracellular
753 polymeric substances in UASB and EGSB reactors treating medium and low
754 concentrated wastewaters. Water Sci. Technol. 48, 41–49.

755 Ramakrishnan, A., Gupta, S.K., 2006. Anaerobic biogranulation in a hybrid reactor
756 treating phenolic waste. J. Hazard. Mater. 137, 1488–1495.
757 doi:10.1016/j.jhazmat.2006.04.034

758 Rotaru, A.-E., Shrestha, P.M., Liu, F., Shrestha, M., Shrestha, D., Embree, M., Zengler,
759 K., Wardman, C., Nevin, K.P., Lovley, D.R., 2014. A new model for electron flow
760 during anaerobic digestion: direct interspecies electron transfer to Methanosaeta
761 for the reduction of carbon dioxide to methane. Energy Environ. Sci. 7, 408–415.
762 doi:10.1039/C3EE42189A

763 Schink, B., Kremer, D.R., Hansen, T.A., 1987. Pathway of propionate formation from
764 ethanol in Pelobacter propionicus. Arch. Microbiol. 147, 321–327.
765 doi:10.1007/BF00406127

766 Schmidt, J.E.E., Ahring, B.K., 1994. Extracellular polymers in granular sludge from
767 different upflow anaerobic sludge blanket (UASB) reactors. Appl. Microbiol.
768 Biotechnol. 42, 457–462. doi:10.1007/BF00902757

769 Shen, L., Zhao, Q., Wu, X., Li, X., Li, Q., Wang, Y., 2016. Interspecies electron
770 transfer in syntrophic methanogenic consortia: From cultures to bioreactors.
771 Renew. Sustain. Energy Rev. 54, 1358–1367. doi:10.1016/j.rser.2015.10.102

772 Sheng, G.P., Yu, H.Q., Li, X.Y., 2010. Extracellular polymeric substances (EPS) of
773 microbial aggregates in biological wastewater treatment systems: A review.
774 Biotechnol. Adv. 28, 882–894. doi:10.1016/j.biotechadv.2010.08.001

775 Show, K.Y., Wang, Y., Foong, S.F., Tay, J.H., 2004. Accelerated start-up and enhanced
776 granulation in upflow anaerobic sludge blanket reactors. Water Res. 38, 2292–

2303. doi:10.1016/j.watres.2004.01.039

Shrestha, P.M., Malvankar, N.S., Werner, J.J., Franks, A.E., Elena-Rotaru, A., Shrestha, M., Liu, F., Nevin, K.P., Angenent, L.T., Lovley, D.R., 2014. Correlation between microbial community and granule conductivity in anaerobic bioreactors for brewery wastewater treatment. Bioresour. Technol. 174, 306–310. doi:10.1016/j.biortech.2014.10.004

Siggins, A., Enright, A.M., O'Flaherty, V., 2011. Temperature dependent (37-15^{o}C) anaerobic digestion of a trichloroethylene-contaminated wastewater. Bioresour. Technol. 102, 7645–7656. doi:10.1016/j.biortech.2011.05.055

Stams, A.J.M., Sousa, D.Z., Kleerebezem, R., Plugge, C.M., 2012. Role of syntrophic microbial communities in high-rate methanogenic bioreactors. Water Sci. Technol. 66, 352–362. doi:10.2166/wst.2012.192

Strand, S.P., Vårum, K.M., Østgaard, K., 2003. Interactions between chitosans and bacterial suspensions: Adsorption and flocculation. Colloids Surfaces B Biointerfaces 27, 71–81. doi:10.1016/S0927-7765(02)00043-7

Thanh, N.T., Watari, T., Thao, T.P., Hatamoto, M., Tanikawa, D., Syutsubo, K., Fukuda, M., Tan, N.M., Anh, T.K., Yamaguchi, T., Huong, N.L., 2016. Impact of aluminum chloride on process performance and microbial community structure of granular sludge in an upflow anaerobic sludge blanket reactor for natural rubber processing wastewater treatment. Water Sci. Technol. 74, 500–507. doi:10.2166/wst.2016.229

Uyanik, S., Sallis, P.J., Anderson, G.K., 2002. The effect of polymer addition on granulation in an anaerobic baffled reactor (ABR). Part I: process performance. Water Res. 36, 933–943. doi:10.1016/S0043-1354(01)00315-3

van Lier, J.B., 2008. High-rate anaerobic wastewater treatment: Diversifying from end-of-the-pipe treatment to resource-oriented conversion techniques. Water Sci. Technol. 57, 1137–1148. doi:10.2166/wst.2008.040

van Lier, J.B., Zee, F.P., Frijters, C.T.M.J., Ersahin, M.E., 2015. Celebrating 40 years anaerobic sludge bed reactors for industrial wastewater treatment. Rev. Environ. Sci. Bio/Technology 14, 681–702. doi:10.1007/s11157-015-9375-5

Vavilin, V.A., Qu, X., Mazéas, L., Lemunier, M., Duquennoi, C., He, P., Bouchez, T., 2008. Methanosarcina as the dominant aceticlastic methanogens during mesophilic anaerobic digestion of putrescible waste. Antonie van Leeuwenhoek, Int. J. Gen. Mol. Microbiol. 94, 593–605. doi:10.1007/s10482-008-9279-2

Wang, D., Han, H., Han, Y., Li, K., Zhu, H., 2017. Enhanced treatment of Fischer-Tropsch (F-T) wastewater using the up-flow anaerobic sludge blanket coupled with bioelectrochemical system: Effect of electric field. Bioresour. Technol. 232, 18–26. doi:10.1016/j.biortech.2017.02.010

Wiegant, W.M., 1987. The "spaghetti theory" on anaerobic sludge formation, or the inevitability of granulation, in: Lettinga, G., A.J.B. Zehnder, J.T.C. Grotenhuis, Pol, L.W.H. (Eds.), Granular Anaerobic Sludge, Microbiology and Technology. The Netherlands: Pudoc. Wageningen, pp. 146–152.

819 Yang, R., Li, H., Huang, M., Yang, H., Li, A., 2016. A review on chitosan-based
820 flocculants and their applications in water treatment. Water Res. 95, 59–89.
821 doi:10.1016/j.watres.2016.02.068

822 Yanti, H., Wikandari, R., Millati, R., Niklasson, C., Taherzadeh, M.J., 2014. Effect of
823 ester compounds on biogas production: beneficial or detrimental? Energy Sci. Eng.
824 2, 22–30. doi:10.1002/ese3.29

825 Zhang, H., Banaszak, J.E., Parameswaran, P., Alder, J., Krajmalnik-Brown, R.,
826 Rittmann, B.E., 2009. Focused-Pulsed sludge pre-treatment increases the bacterial
827 diversity and relative abundance of acetoclastic methanogens in a full-scale
828 anaerobic digester. Water Res. 43, 4517–4526. doi:10.1016/j.watres.2009.07.034

829 Zhang, L., Feng, X., Zhu, N., Chen, J., 2007. Role of extracellular protein in the
830 formation and stability of aerobic granules. Enzyme Microb. Technol. 41, 551–
831 557. doi:10.1016/j.enzmictec.2007.05.001

832 Zhao, Z., Zhang, Y., Yu, Q., Dang, Y., Li, Y., Quan, X., 2016. Communities stimulated
833 with ethanol to perform direct interspecies electron transfer for syntrophic
834 metabolism of propionate and butyrate. Water Res. 102, 475–484.
835 doi:10.1016/j.watres.2016.07.005

836 Zhou, W., Imai, T., Ukita, M., Sekine, M., Higuchi, T., 2006. Triggering forces for
837 anaerobic granulation in UASB reactors. Process Biochem. 41, 36–43.
838 doi:10.1016/j.procbio.2005.02.029

839

840

841 **Table 1.** Operational parameters of UASB reactors during the granulation experiment.

Operational day	Phase I 0 – 22			Phase II 23 – 89			Phase III 90 – 219		
	R1	R2	R3	R1	R2	R3	R1	R2	R3
OLR (kg COD m^{-3} d^{-1})	0.3 – 0.6	0.3 – 0.6	0.3 – 0.6	2.3	2.3	4	2.3 – 20	2.3 – 20	4 – 20
Influent COD (g L^{-1})	2.3 – 4.5	2.3 – 4.5	2.3 – 4.5	3.0	3.0	3.0	5.0 – 7.6	5.0 – 7.6	4.0 – 5.3
Influent E2P (mg L^{-1})	110 – 220	110 – 220	110 – 220	145	145	145	240 – 370	240 – 370	190 – 260
u (m h^{-1})	1	1	0.1	1	1	0.1	0.1 – 0.2	0.1 – 0.2	0.1 – 0.2

842

Table 2. Percentage of particles larger than 300 μm (consider as granules) over time in all reactors.

		Operational time (day)											
		Phase I				Phase II			Phase III				
				0	22	23	54	89	90	112	131	169	190	219
Granules (%)	R1	1st Chitosan Addition Recirculation ON		0.3	3.0	2nd Chitosan Addition	4.9	4.9	Recirculation OFF	4.9	18.1	25.4	33.0	42.0
	R2			0.3	4.0		6.3	8.5		22.7	25.0	40.2	56.4	54.0
	R3		Rec. OFF	0.3	6.8		22.2	21.9		24.5	30.1	57.3	65.7	64.7

848 **Table 3.** Extracellular polymer content of the sludge samples from the reactors during
849 the study.
850

	EPS (mg g VSS^{-1})	Polysaccharides			Proteins			Total EPS		
	Day	R1	R2	R3	R1	R2	R3	R1	R2	R3
Phase I	0	5.7	5.7	5.7	2.4	2.4	2.4	8.1	8.1	8.1
	18	1.4	9.5	2.2	2.3	3.9	4.2	3.8	13.4	6.3
Phase II	54	16.0	14.5	17.2	14.0	40.9	36.8	30.0	55.3	54.0
	89	2.6	4.0	9.2	26.5	49.7	37.4	29.1	53.7	46.5
Phase III	112	7.1	8.2	4.1	19.1	48.4	30.3	26.2	56.6	34.3
	131	7.7	19.8	10.8	49.2	44.8	55.6	56.9	64.6	66.4
	190	8.3	21.1	30.4	81.3	101.9	168.3	89.5	123.0	198.7
	219	11.2	24.0	20.7	94.2	158.2	131.3	105.5	182.3	152.0

851

852 **Table 4.** SMA of the granular sludge of each reactor after 219 days of operation.

	SMA (NmL CH_4 g VSS^{-1} d^{-1})			
	Ethanol	Ethyl Acetate	E2P	Mixture
R1: Control	277.8 ± 8.0	265.5 ± 22.4	66.7 ± 5.2	245.2 ± 3.0
R2	434.5 ± 2.4	370.0 ± 14.0	73.3 ± 2.2	390.7 ± 4.6
R3	488.6 ± 4.1	386.9 ± 16.0	79.9 ± 1.9	439.9 ± 1.9

853

854 **Table 5.** Phylogenic affiliation of bacterial and archaeal sequenced bands from DGGE
855 profiles (Fig. 6).

DGGE band	Closest organism (accession. version number)	Similarity %	Phylogenetic group (phylum/order)
B1	*Paludibaculum fermentans (NR_134120.1)*	95	*Bacteroidetes/Bacteroidales*
B2	*Catalinimonas niigatensis (NR_133994.1)*	92	*Acidobacteria*
B3	*Hydrogenophaga luteola (NR_145548.1)*	100	*Proteobacteria/Burkholderiales*
B4	*Desulfovirgula thermocuniculi (NR_043640.1)*	88	*Firmicutes/Thermoanaerobacteriales*
B5	*Capnocytophaga cynodegmi (NR_043063.1)*	94	*Bacteroidetes/Flavobacteriales*
B6	*Flavobacterium aquaticum (NR_108893.1)*	96	*Bacteroidetes/Flavobacteriales*
B7	*Geobacter psychrophilus (NR_043075.1)*	95	*Proteobacteria/Desulfuromonadales*
B8	*Clostridium limosum (NR_104825.1)*	90	*Firmicutes/Clostridiales*
B9	*Capnocytophaga sputigena (NR_113564.1)*	88	*Bacteroidetes/Flavobacteriales*
B10	*Pelobacter propionicus (NR_074975.1)*	93	*Proteobacteria/Desulfuromonadales*
B11	*Smithella propionica (NR_024989.1)*	92	*Proteobacteria/Syntrophobacterales*
B12	*Treponema caldarium (NR_074757.1)*	91	*Spirochaetes/Spirochaetales*
B13	*Capnocytophaga granulosa (NR_044777.1)*	92	*Bacteroidetes/Flavobacteriales*
B14	*Flavobacterium branchiicola (NR_145953.1)*	85	*Bacteroidetes/Flavobacteriales*
B15	*Trichococcus pasteurii (NR_036793.2)*	98	*Firmicutes/Lactobacillales*
B16	*Geobacter chapellei (NR_025982.1)*	95	*Proteobacteria/Desulfuromonadales*
B17	*Capnocytophaga granulosa (NR_044777.1)*	92	*Bacteroidetes/Flavobacteriales*
A1	*Methanocorpusculum labreanum (NR_074173.1)*	100	*Methanomicrobiales/Methanocorpusculaceae*
A2	*Methanospirillum hungatei (NR_074177.1)*	79	*Methanomicrobiales/ Methanospirillaceae*
A3	*Methanosaeta concilii (NR_102903.1)*	100	*Methanosarcinales/Methanosaetaceae*
A4	*Methanosaeta thermophila (NR_074214.1)*	96	*Methanosarcinales/Methanosaetaceae*
A5	*Methanosaeta harundinacea (NR_043203.1)*	99	*Methanosarcinales/Methanosaetaceae*
A6	*Methanobacterium beijingense (NR_028202.1)*	99	*Methanobacteriales/Methanobacteriaceae*
A7	*Methanosarcina mazei (NR_041956.1)*	100	*Methanosarcinales/ Methanosarcinaceae*
A8	*Methanosaeta harundinacea (NR_043203.1)*	98	*Methanosarcinales/Methanosaetaceae*
A9	*Methanosaeta concilii (NR_102903.1)*	100	*Methanosarcinales/Methanosaetaceae*

856

Figure captions

Figure 1. Schematic diagram of experimental set-up.

Figure 2. a) Applied Organic Loading Rate (▬) and COD removal efficiency (●,○,▲) of the reactors during the experiment. **b)** VFA concentration in the effluent of the reactors.

Figure 3. Variation of the applied E2P Organic Loading Rate (▬) and E2P removal efficiency (●,○,▲) of the reactors with time.

Figure 4. Evolution of the particle size and distribution over time in all reactors.

Figure 5. SEM images: Morphology of the granules after 219 days. **a.** Control reactor (R1), **b**. chitosan-assisted reactor (R3), **c.** Magnification of granules in R1, **d**. Magnification of granules in R3.

Figure 6. Variation with time of the DGGE profiles of biomass samples from the three reactors. a) Bacterial DGGE profiles, b) Archeal DGGE profiles.

Figure 7. Heatmap distribution of the most abundant genera (relative abundance > 0.1% at least in one sample) of biomass samples from the inoculum and the three reactors.

Figure1

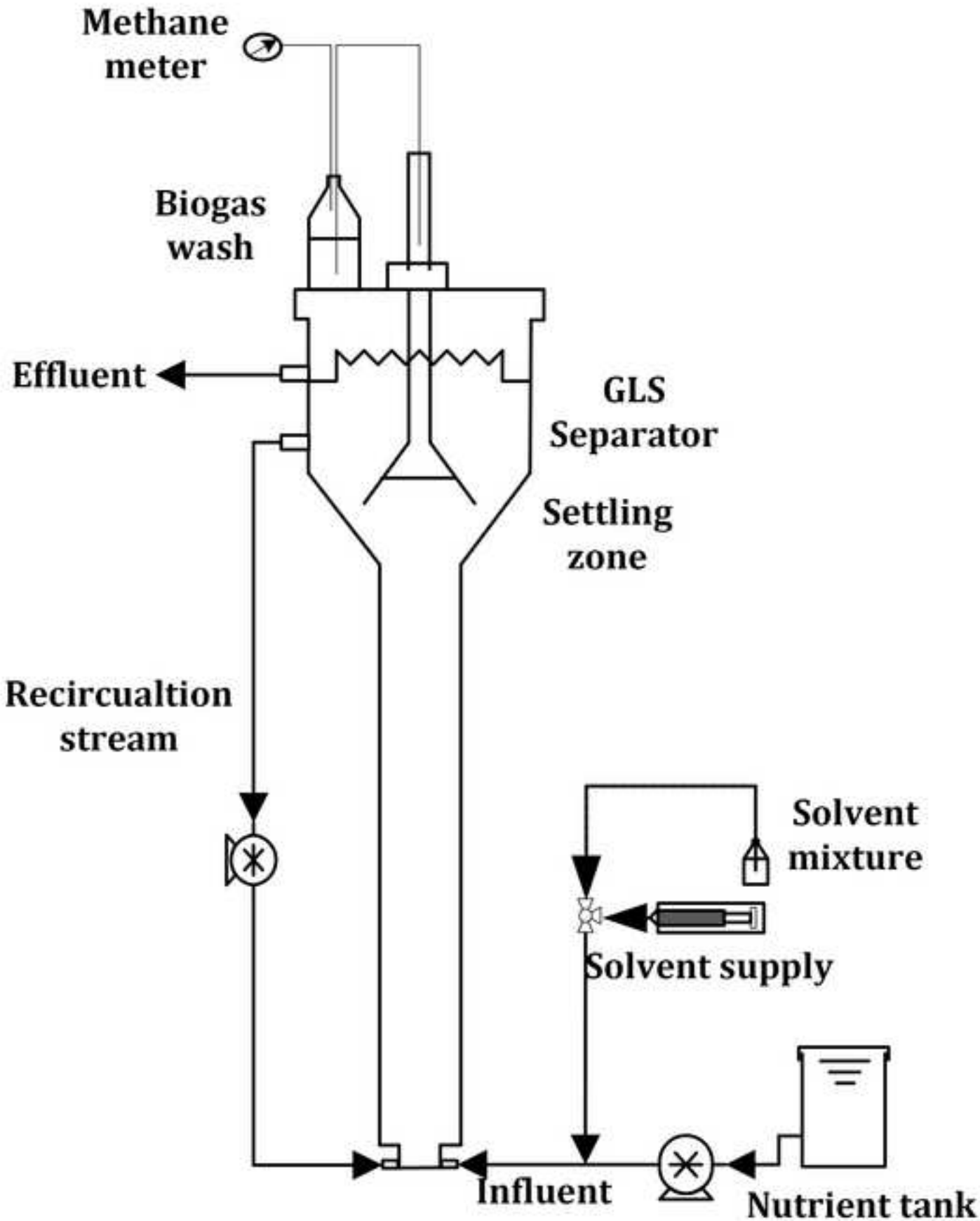
Methane meter
Biogas wash
Effluent
GLS Separator
Settling zone
Recircualtion stream
Solvent mixture
Solvent supply
Influent
Nutrient tank

Figure 2

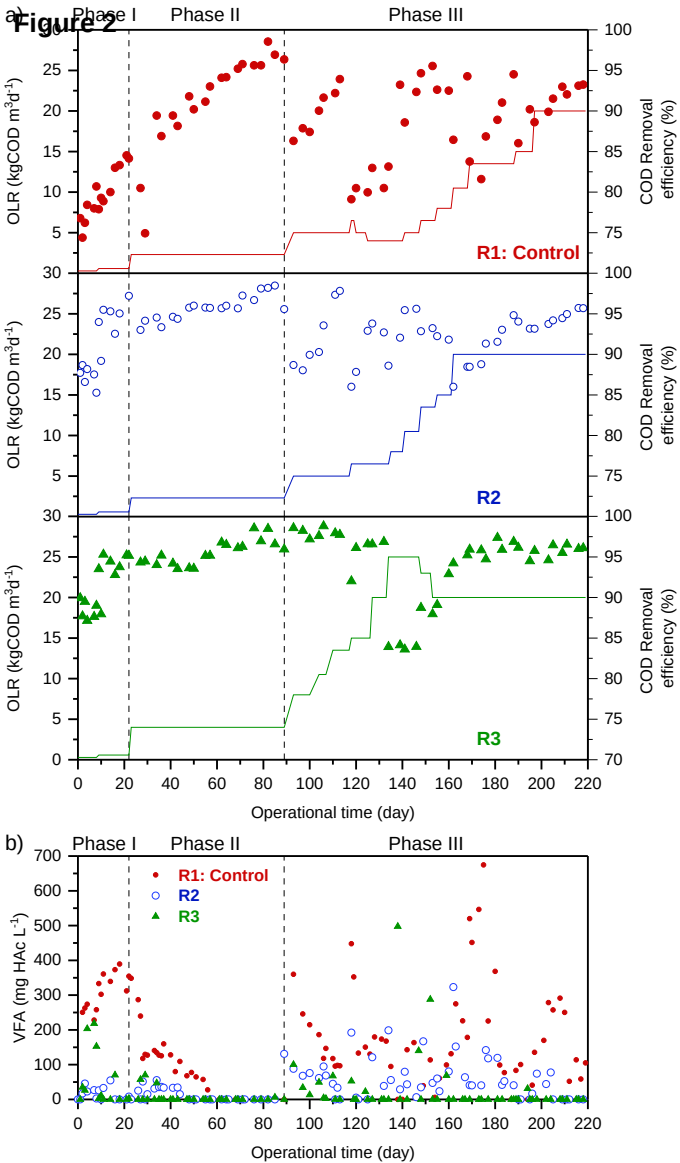
a)
Phase I
Phase II
Phase III
OLR (kgCOD m3d-1)
COD Removal efficiency (%)
R1: Control
R2
R3
Operational time (day)
b)
VFA (mg HAc L-1)
R1: Control
R2
R3
Operational time (day)

Figure3

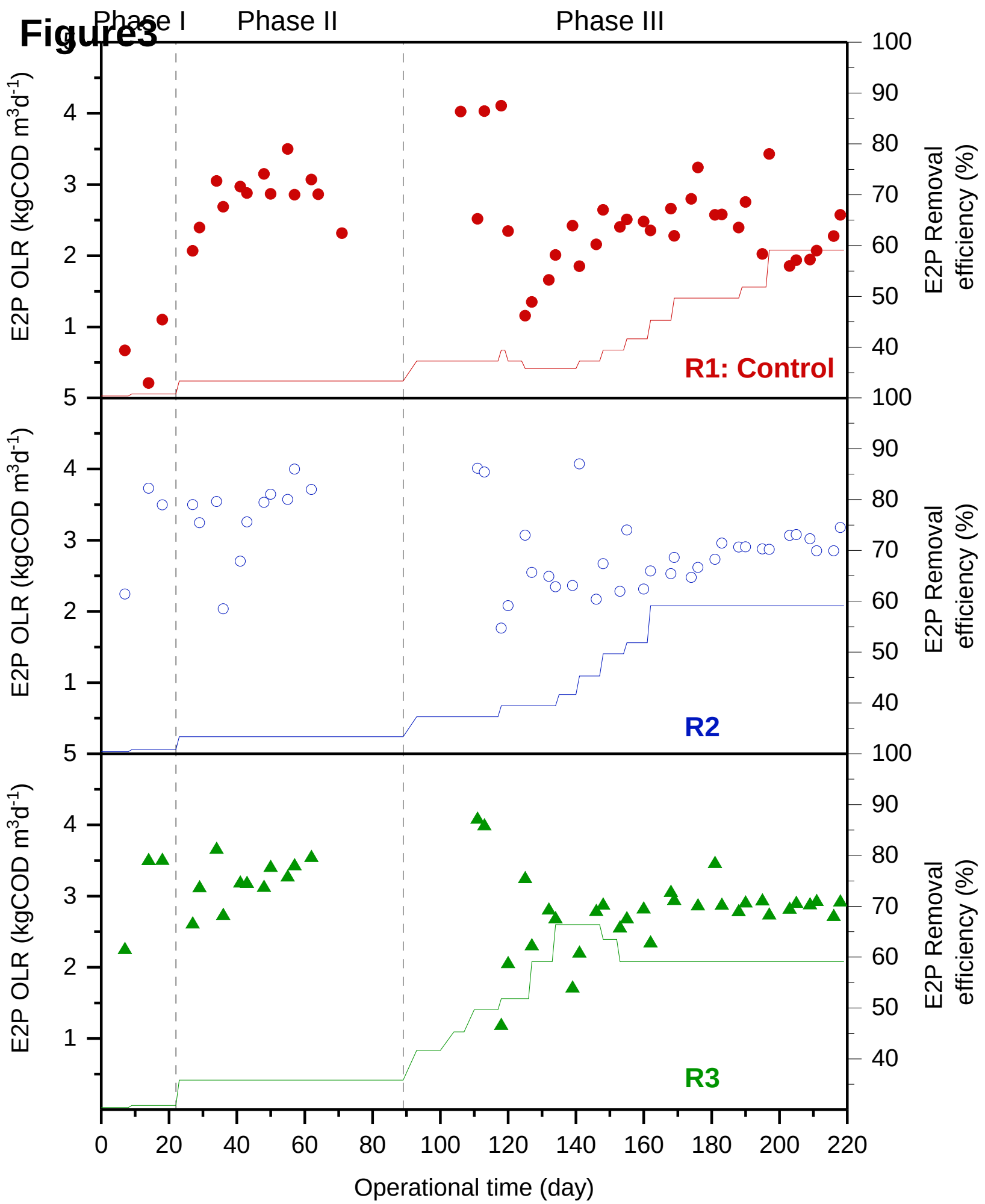
Phase I
Phase II
Phase III
E2P OLR (kgCOD m3d-1)
E2P Removal efficiency (%)
R1: Control
R2
R3
Operational time (day)
0
20
40
60
80
100
120
140
160
180
200
220
1
2
3
4
5
40
50
60
70
80
90
100

Figure4

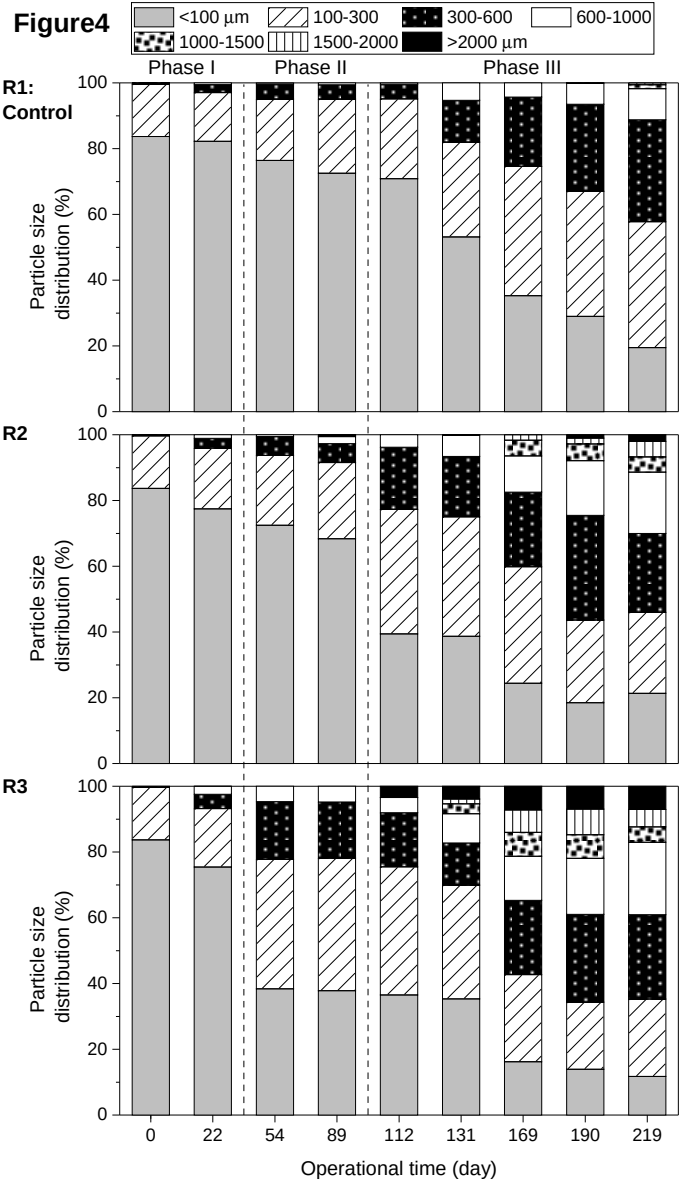
<100 μm
100-300
300-600
600-1000
1000-1500
1500-2000
>2000 μm
Phase I
Phase II
Phase III
R1: Control
R2
R3
Particle size distribution (%)
0
20
40
60
80
100
0
22
54
89
112
131
169
190
219
Operational time (day)

Figure5

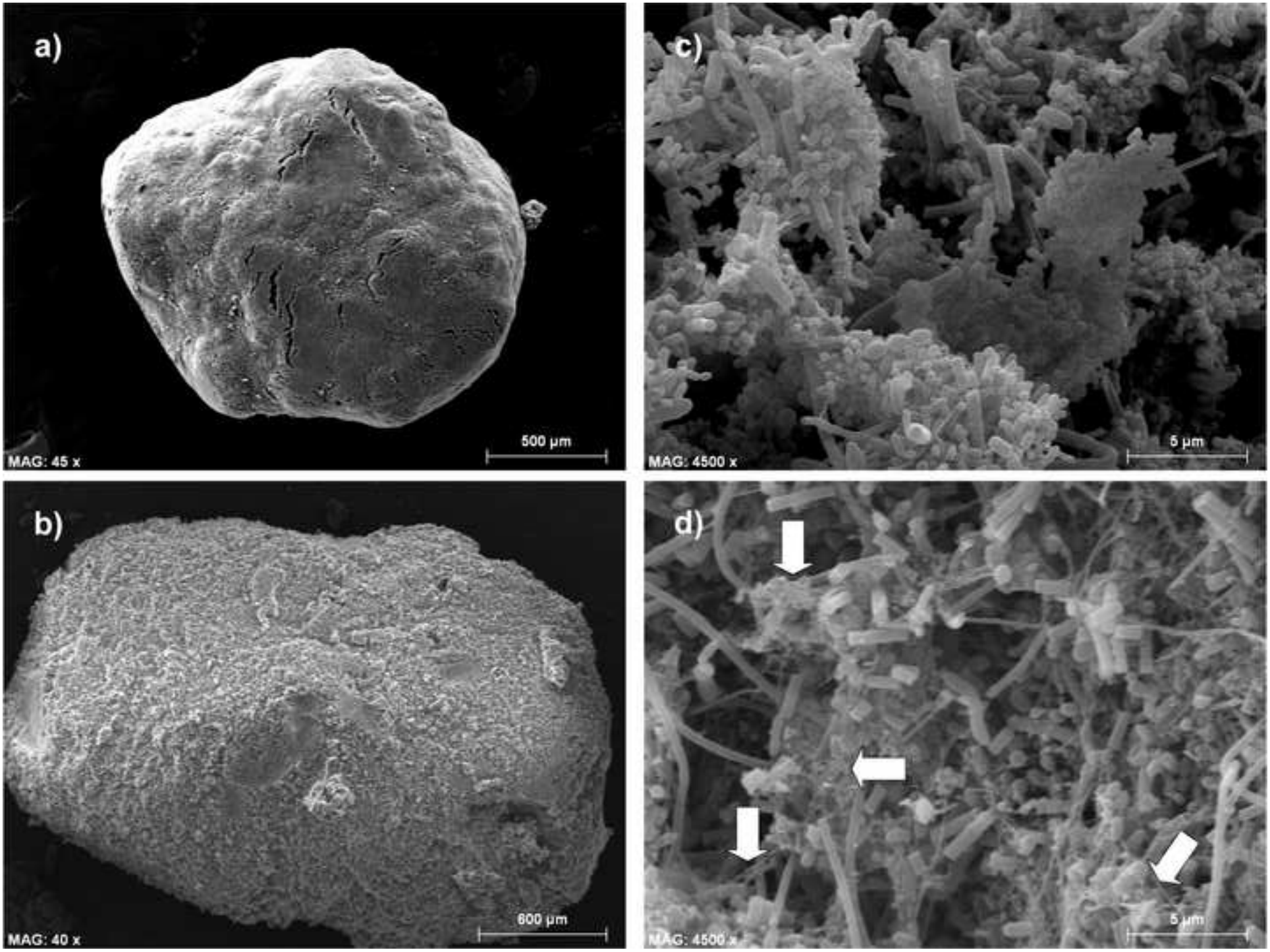

Figure 6

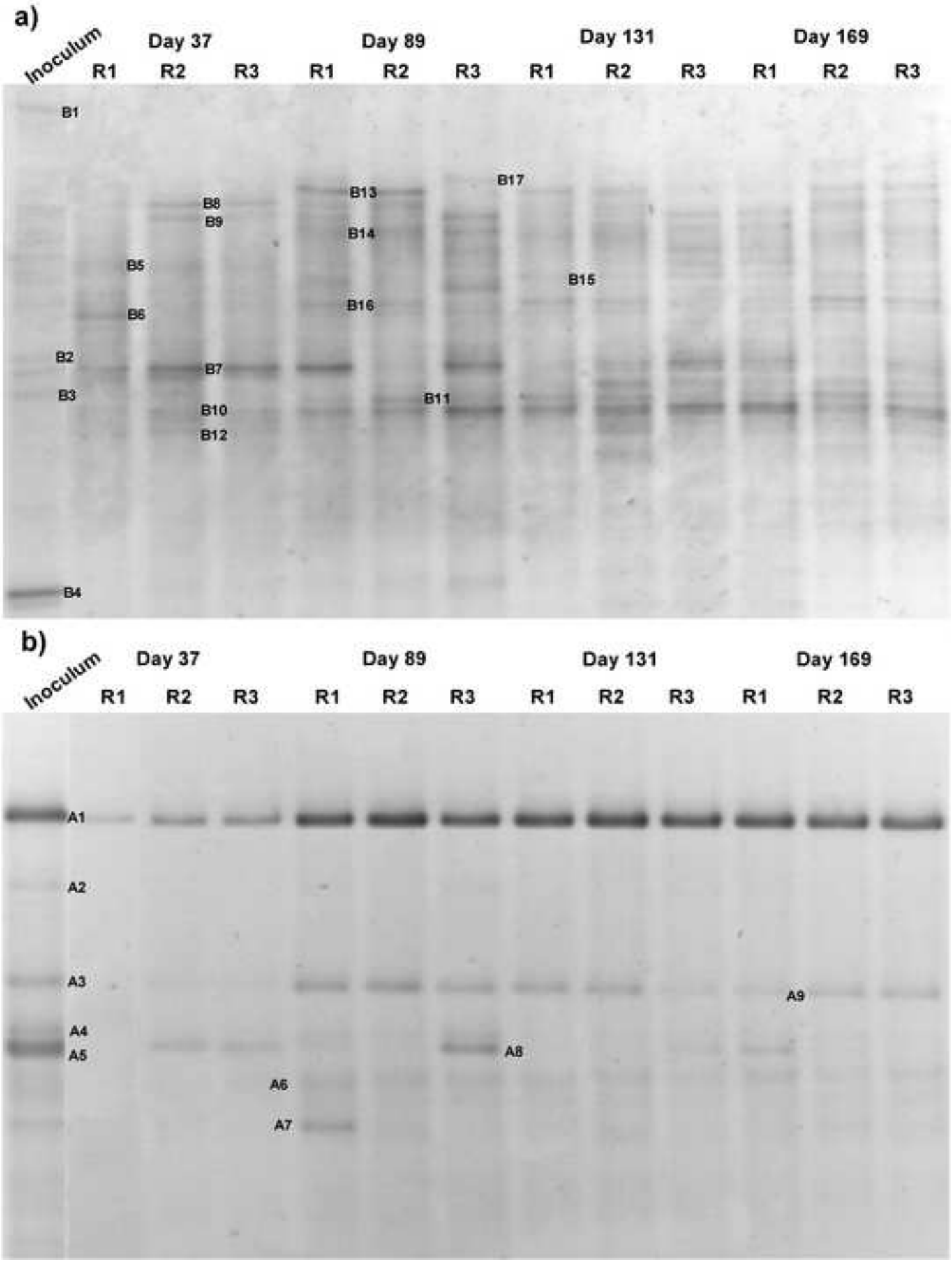
a)
Inoculum
Day 37
Day 89
Day 131
Day 169
R1
R2
R3
B1
B2
B3
B4
B5
B6
B7
B8
B9
B10
B11
B12
B13
B14
B15
B16
B17
b)
Inoculum
Day 37
Day 89
Day 131
Day 169
R1
R2
R3
A1
A2
A3
A4
A5
A6
A7
A8
A9

Figure7

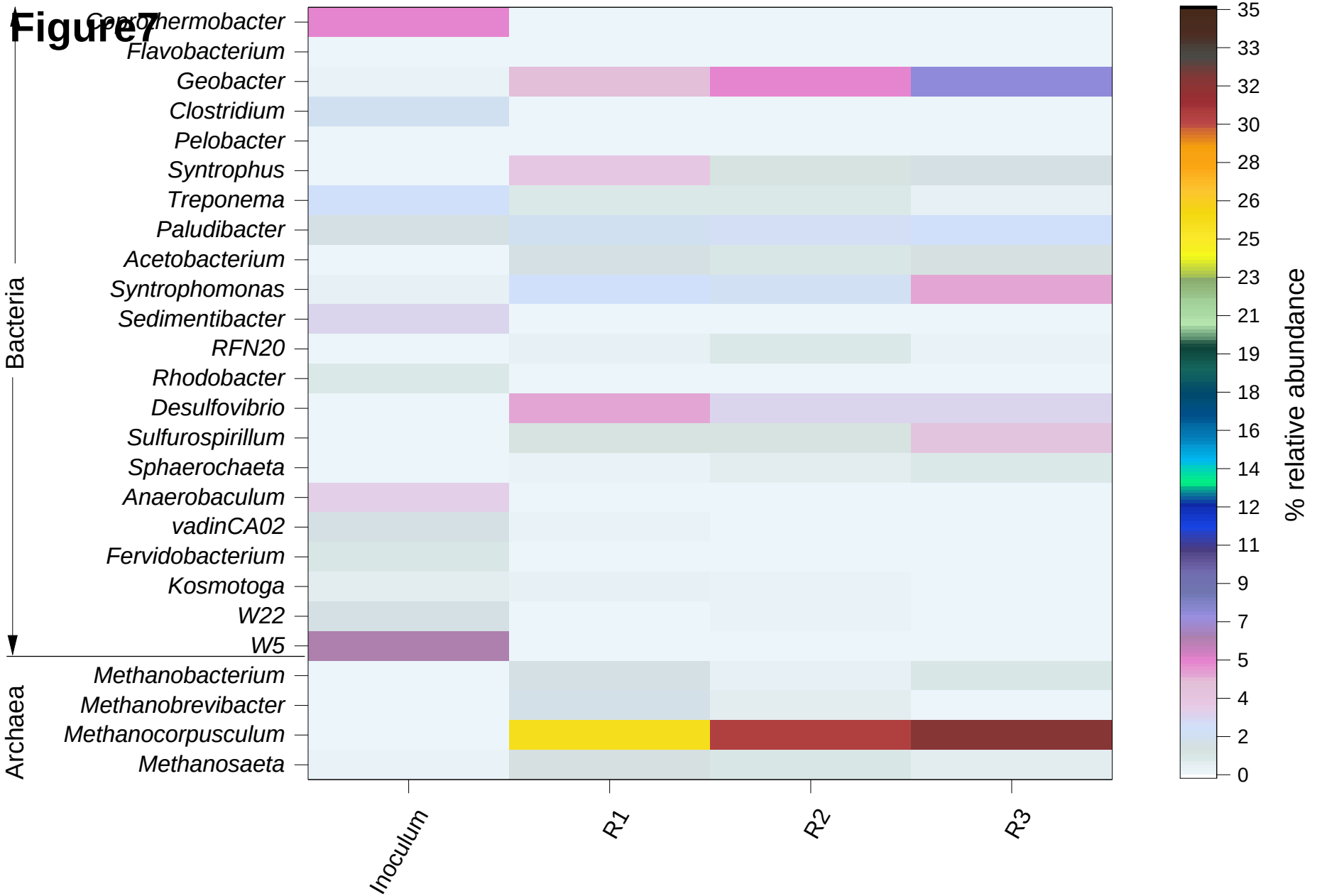
Caldithermobacter
Flavobacterium
Geobacter
Clostridium
Pelobacter
Syntrophus
Treponema
Paludibacter
Acetobacterium
Syntrophomonas
Sedimentibacter
RFN20
Rhodobacter
Desulfovibrio
Sulfurospirillum
Sphaerochaeta
Anaerobaculum
vadinCA02
Fervidobacterium
Kosmotoga
W22
W5
Methanobacterium
Methanobrevibacter
Methanocorpusculum
Methanosaeta
Bacteria
Archaea
Inoculum
R1
R2
R3
35
33
32
30
28
26
25
23
21
19
18
16
14
12
11
9
7
5
4
2
0
% relative abundance

Supplementary material

Equations to calculate RE_{COD} and RE_{E2P}:

1- The COD removal efficiency was calculated as follows:

$$RE_{COD}\ (\%) = 1 - \frac{COD_{effluent}}{COD_{influent}}$$

where $COD_{effluent}$, is soluble COD concentration, measured according to Standard Methods, and $COD_{influent}$, is the COD concentration in the influent, calculated according to the injected mass rate (g d^{-1}) and the composition of the mixture of ethanol, ethyl acetate and 1-ethoxy-2 propanol, using their respective theoretical factors for the conversion from g L^{-1} to g COD L^{-1} (2.08 g COD g Ethanol^{-1}, 1.82 g COD g Ethyl Acetate^{-1} and 2.15 g COD g E2P^{-1}), and the wastewater volumetric flowrate fed (L d^{-1}).

2- The removal efficiency of the solvent E2P was calculated as follows:

$$RE_{E2P}(\%) = 1 - \frac{C_{E2P,effluent}}{C_{E2P,influent}}$$

being $C_{E2P,effluent}$, the concentration of the solvent as g E2P L^{-1}, which was measured by gas chromatography (as explained in Materials and Methods), and $C_{E2P,influent}$ (g E2P L^{-1}), the concentration of E2P in the influent calculated by the mass rate injected of E2P (g E2P d^{-1}) and the wastewater volumetric flowrate fed (L d^{-1}).

Table Sup1. Macro- and micro-nutrients supplementation.

Macro-nutrients	mg g COD^{-1}	Micro-nutrients	mg g COD^{-1}
NH_4Cl	25.5	$FeCl_3 \cdot 6H_2O$	0.42
$(NH_4)_2HPO_4$	14.2	H_3BO_3	0.11
KCl	2.4	$ZnSO_4 \cdot 7H_2O$	0.01
Yeast extract	7.5	$CuCl_2 \cdot 2H_2O$	0.01
Mg^{+2} as $MgCl_2 \cdot 6H_2O$	40 mg Mg L^{-1}	$MnCl_2 \cdot 4H_2O$	0.14
Ca^{+2} as $CaCl_2 \cdot 2H_2O$	150 mg Ca L^{-1}	$(NH_4)6Mo_7O_{24} \cdot 4H_2O$	0.06
		Al_2O_3	0.06
		$CoCl_2 \cdot 6H_2O$	0.16
		$NiSO_4 \cdot 6H_2O$	0.04
		$EDTANa_2$	0.1

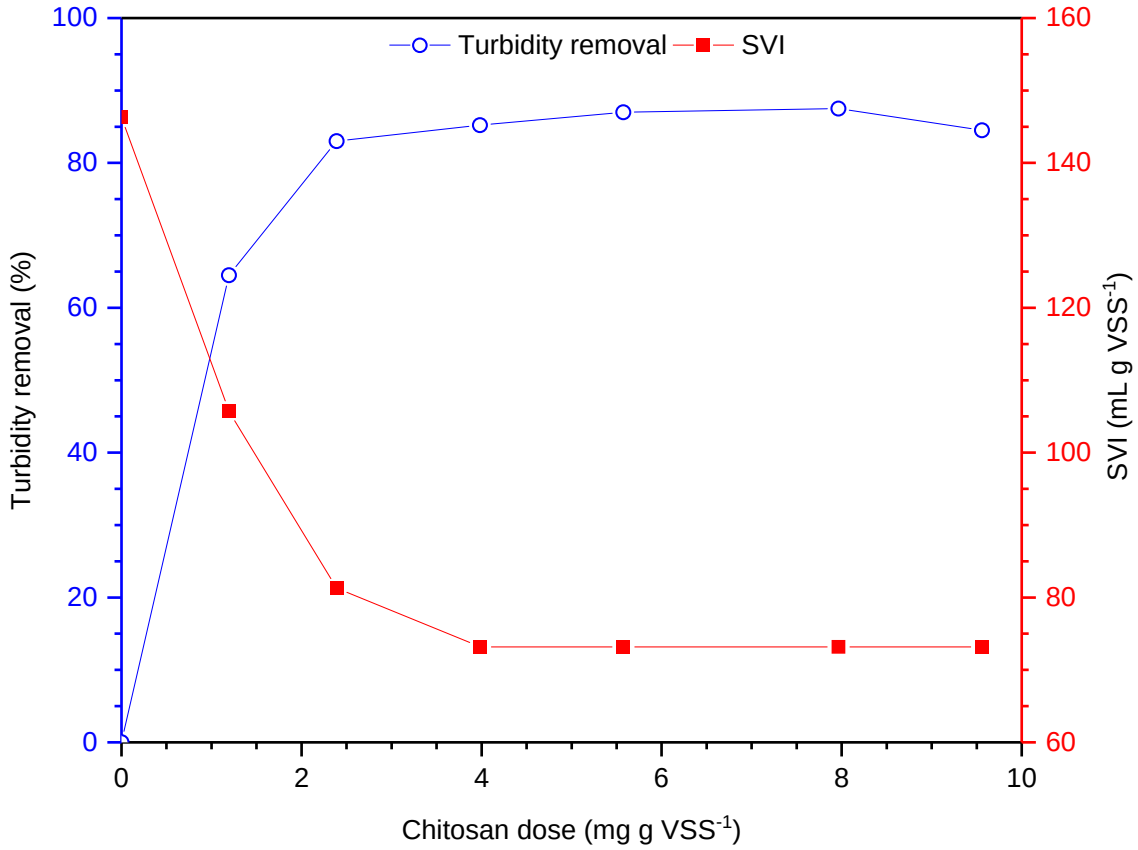

Figure Sup1. Variations in the turbidity and sludge volume index (SVI) at different doses of chitosan applied to the inoculum.

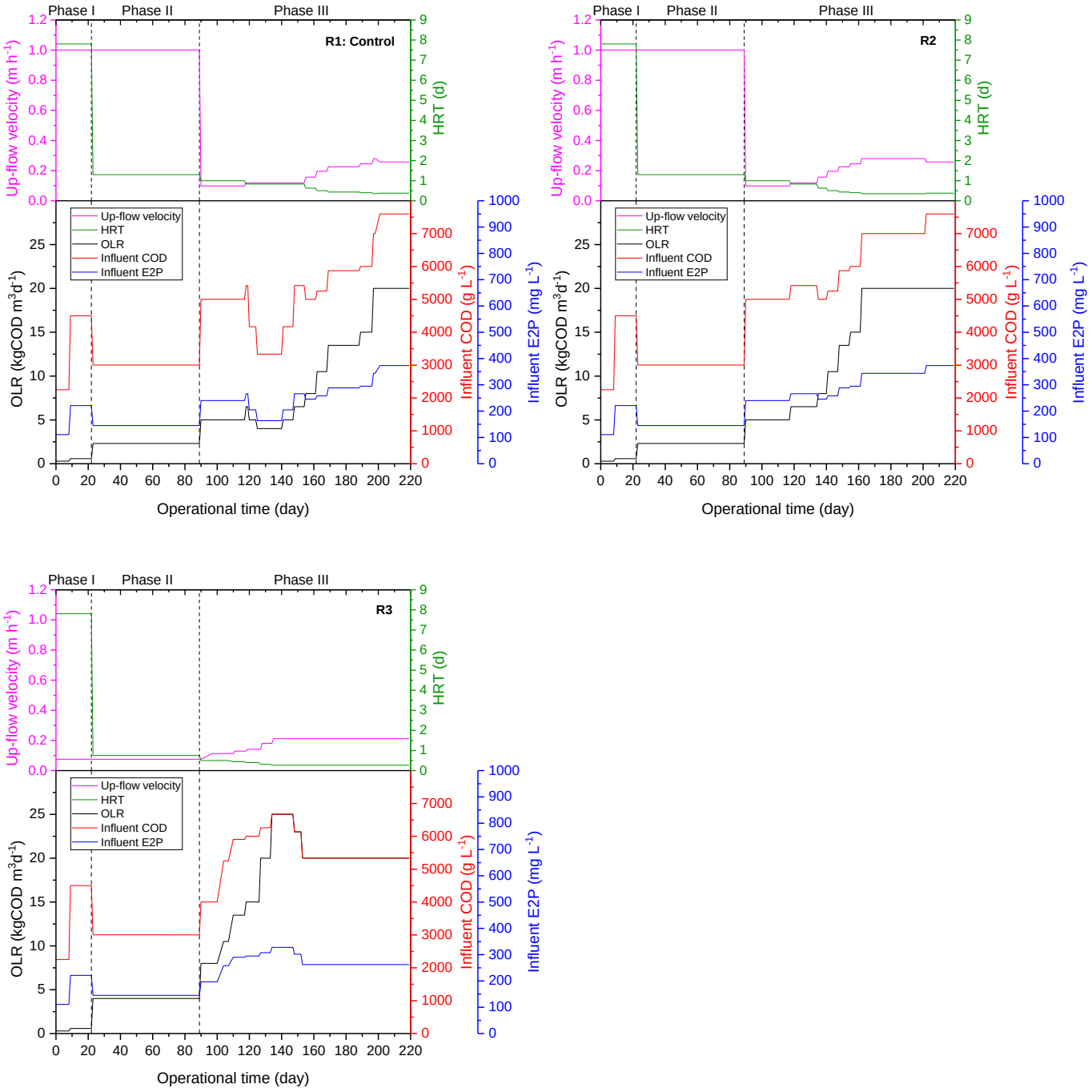

Figure Sup2. Changes of the operational parameters over time in the three UASB reactors during the granulation experiment.

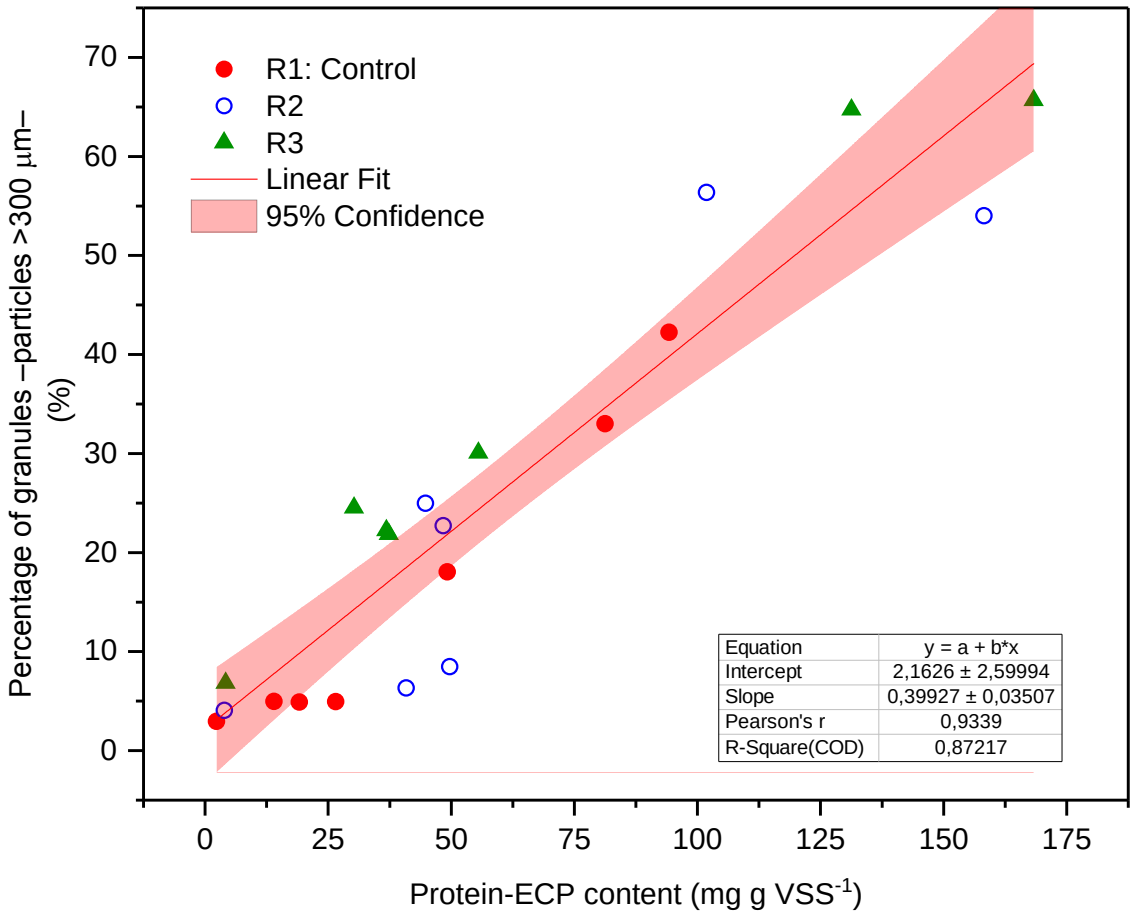

Figure Sup3. Variations in the percentage of granules (particles >300µm) with the protein-ECP content in the three reactors.

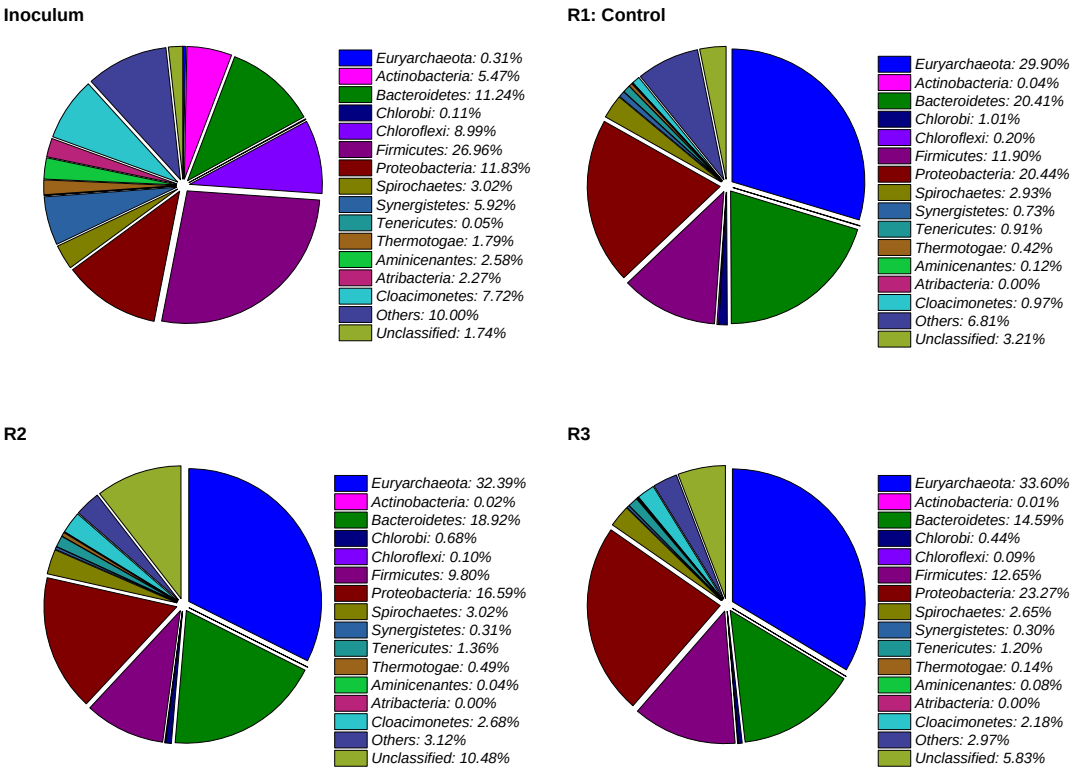

Figure Sup4. Microbial distribution at phylum-level of the inoculum and the samples of the three UASB at day 169.